

**BULGARIAN ACADEMY OF SCIENCES
INSTITUTE OF POLYMERS**

SELIN ERDINCH KYUCHYUK-HYUSEIN

**ELECTROSPUN FIBERS WITH CORE-SHEATH
ARCHITECTURE BASED ON POLY(ETHYLENE
OXIDE), A BIODEGRADABLE ALIPHATIC
POLYESTER AND BEESWAX**

DISSERTATION ABSTRACT

**presented for acquisition of
the Educational and scientific degree "Doctor"**

Sofia, 2025

BULGARIAN ACADEMY OF SCIENCES

INSTITUTE OF POLYMERS

SELIN ERDINCH KYUCHYUK-HYUSEIN

**ELECTROSPUN FIBERS WITH CORE-SHEATH
ARCHITECTURE BASED ON POLY(ETHYLENE
OXIDE), A BIODEGRADABLE ALIPHATIC
POLYESTER AND BEESWAX**

DISSERTATION ABSTRACT

**presented for acquisition of
the Educational and scientific degree "Doctor"**

Professional field: 4.2. Chemical Sciences

Specialty: Polymers and Polymeric Materials

Scientific Supervisors: Assoc. Prof. Dilyana Paneva, DSc

Prof. Iliya Rashkov, DSc,

Corresponding Member of BAS

Sofia, 2025

The dissertation thesis was discussed and admitted for defense at a meeting of the Colloquium of the Institute of Polymers – Bulgarian Academy of Sciences.

The dissertation is presented on 148 pages, includes 70 figures and 123 references. The results have been published in five scientific articles and reported at 5 scientific conferences.

The defense of the dissertation thesis will take place on..... at h in the conference hall of the Institute of Polymers – Bulgarian Academy of Sciences at a meeting of the Scientific Jury.

The defense-related materials are available at the office of the Institute of Polymers – BAS, Sofia, Akad. G. Bonchev St., Block 103B.

Author: Selin Erdinch Kyuchyuk-Hyusein

Title: Electrospun fibers with core-sheath architecture based on poly(ethylene oxide), a biodegradable aliphatic polyester and beeswax

The studies summarized in the dissertation were performed in the Laboratory of Bioactive Polymers, Scientific Department Polymer Biomaterials, Institute of Polymers – Bulgarian Academy of Sciences. A Part of the investigations were performed within the framework of contract KP-06-H39/13/2019, funded by the Bulgarian National Science Fund. Some of the results were obtained using equipment under contract D01-322/2023 within the INFRAMAT project (part of the National Roadmap for Research Infrastructure), financially supported by the Ministry of Education and Science of the Republic of Bulgaria.

The research is part of the long-standing systematic investigations of the Laboratory in the field of innovative electrospun micro- and nanofibrous materials with demonstrated potential for applications in medicine and agropharmacy.

ACKNOWLEDGMENTS

I would like to express my gratitude to the Management of the Institute of Polymers – BAS and to the Director, Corresponding Member Prof. D.Sc. Petar Petrov, for granting me the opportunity to be a doctoral student on an independent study program and for the support provided throughout the entire period of my training.

I am thankful to Mrs. Neli Velinova for her assistance and correctness in organizational and administrative matters, as well as for her constant readiness to provide help.

I would like to express my deep appreciation to Corresponding Member Prof. D.Sc. Iliya Rashkov, who was always available and willing to help. He was my true mentor and source of inspiration. I owe special gratitude to Assoc. Prof. D.Sc. Dilyana Paneva, whose guidance and valuable advice helped me overcome numerous challenges during my work. I thank them both for their support and patience throughout the entire research process.

I sincerely thank Prof. D.Sc. Nevena Manolova for her rigor and attention to every detail, as well as for the invaluable guidance that contributed to the quality and completeness of this dissertation.

I would also like to express my heartfelt gratitude to Prof. Milena Ignatova for her assistance, support, and for sharing her professional experience.

I warmly thank all my colleagues from the Laboratory of Bioactive Active Polymers and from the Institute of Polymers for their support, cooperation, and friendly attitude.

I am deeply grateful to Prof. Daniela Karashanova (Institute of Optical Materials and Technologies, BAS), Prof. Reneta Toshkova and Assoc. Prof. Ani Georgieva (Institute of Experimental Morphology, Pathology and Anthropology with Museum, BAS), Assoc. Prof. Nadya Markova (Institute of Microbiology, BAS), and Assoc. Prof. Mladen Naydenov (Agricultural University – Plovdiv) for their assistance in carrying out the analyses required for the realization of this dissertation.

I would like to thank my family, who have always been by my side with love, patience, and faith in me.

***Dedicated to my colleagues Albena Cherneva (Institute of Microbiology, BAS) and
Yoana Veleva (Institute of Polymers, BAS), whose memory will remain forever in
my heart.***

LIST OF ABBREVIATIONS

AO	Acridine orange
<i>B. amyloliquefaciens</i>	<i>Bacillus amyloliquefaciens</i>
<i>B. cereus</i>	<i>Bacillus cereus</i>
BJ	Normal human skin fibroblasts
<i>C. albicans</i>	<i>Candida albicans</i>
BW	Beeswax
CQ	5-chloro-7-iodo-8-hydroxyquinoline
DMSO	Dimethyl sulfoxide
DSC	Differential scanning calorimetry
<i>E. coli</i>	<i>Escherichia coli</i>
EtBr	Ethidium bromide
<i>F. avenaceum</i>	<i>Fusarium avenaceum</i>
<i>F. graminearum</i>	<i>Fusarium graminearum</i>
FTIR	Fourier-transform infrared spectroscopy
HeLa	Human cervical adenocarcinoma cells
NQ	5-nitro-8-hydroxyquinoline
<i>P. aeruginosa</i>	<i>Pseudomonas aeruginosa</i>
<i>P. chlororaphis</i>	<i>Pseudomonas chlororaphis</i>
<i>P. corrugata</i>	<i>Pseudomonas corrugata</i>
PBS	Poly(butylene succinate)
PCL	Poly(ϵ -caprolactone)
PEO	Poly(ethylene oxide)
PEO600k	PEO with molecular weight 600,000 g/mol
PEO100k	PEO with molecular weight 100,000 g/mol
PLA	Poly(lactide)
PLA259k	PLA with molecular weight 259,000 g/mol
PLA911k	PLA with molecular weight 911,000 g/mol
PHB	Poly(3-hydroxybutyrate)
PLAGA	Poly(D,L-lactide-co-glycolide)
PLDLA	Poly(L-lactide-co-D,L-lactide)
<i>S. aureus</i>	<i>Staphylococcus aureus</i>
SEM	Scanning electron microscopy
SH-4	Human melanoma cells
<i>T. asperellum</i>	<i>Trichoderma asperellum</i>
TGA	Thermogravimetric analysis
TEM	Transmission electron microscopy
THF	Tetrahydrofuran
XPS	X-ray photoelectron spectroscopy
XRD	X-ray diffraction
ZnO	Unmodified zinc oxide
ZnO(Si)	Zinc oxide with silanized surface

The scientific publications presented in the dissertation are given in square brackets as superscripts to each chapter title. The numbering of the publications corresponds to the numbering in the list of the candidate's publications and scientific communications, provided at the end of the dissertation. To avoid errors and omissions, the figures have been taken exactly as they appear in the original publications.

[P №] - indicates a publication of the doctoral candidate;

[PP №] - indicates a scientific communication in the form of a poster presentation involving the doctoral candidate;

[OP №] – indicates a scientific communication in the form of an oral presentation involving the doctoral candidate

The numbering of the chapters and figures in the Dissertation Abstract corresponds to that in the dissertation thesis.

I.INTRODUCTION

In the context of today's global challenges related to healthcare, the environment, and sustainable development, there is a growing need to develop innovative materials with high biocompatibility, controlled biodegradability, and the capacity for precise release of bioactive substances (BAS). One of the most promising approaches in this field is the use of fibrous materials, which possess unique morphological characteristics, a high specific surface area, and the possibility for structural modification.

The fabrication of such micro- and nanofibrous materials relies on the so-called electrohydrodynamic methods. These highly innovative methods enable the preparation of a wide range of materials, including micro- and nanofibers as well as micro- and nanoparticles. The first type of processes is known as electrospinning, while the second is termed electrospraying. The combination of these two techniques opens possibilities for producing fibrous materials "decorated" with micro- or nanoparticles. Noteworthy, the electrospinning offers a remarkably wide range of possibilities for processing polymers, polymer solutions, suspensions, and emulsions. A wide range of polymers can be converted into melts and electrospun. However, such studies are to a great extent constrained by the risk of degradation reactions at elevated temperatures. Conversely, electrospinning from solutions, emulsions, or suspensions can be carried out under mild conditions and offers the advantage of using more environmentally friendly solvent systems. Furthermore, electrospinning of solutions, emulsions, or suspensions enables the incorporation of a wide range of bioactive low- and high-molecular-weight additives. By employing innovative engineering solutions, such as multi-nozzle systems (e.g., centrifugal electrospinning), the process throughput can be increased. Under appropriate experimental conditions - such as optimized polymer concentration, the presence of stabilizers for suspensions and emulsions, and controlled flow rates from the nozzles; fibers with diverse morphologies can be obtained, ranging from smooth, cylindrical, defect-free fibers to fibers exhibiting bead- or spindle-like defects. With respect to more complex internal architectures, such as core-sheath fibers, a coaxial nozzle has been developed. This is the so-called coaxial electrospinning technique. In recent years, successful attempts have been made to produce these valuable structures

by electrospinning of emulsions using a single-nozzle spinneret. However, a review of recent literature revealed certain limitations in emulsion electrospinning, as the stabilization of the emulsions often requires undesirable and environmentally harmful additives. Furthermore, no reports have been found on the preparation of core-double sheath fibers by single-nozzle spinneret electrospinning. Our hypothesis was that such structures could be obtained by appropriate selection of certain biocompatible and biodegradable polymers with optimal molecular weights in combination with beeswax.

Fibers with core-sheath architecture provide a new level of functionality, allowing spatial separation of the components with different chemical and biological roles - for example, a hydrophilic core capable of incorporating and releasing BAS, and a hydrophobic sheath that controls the release kinetics, provides moisture and barrier protection. The existing methods for producing such fibers (most often coaxial electrospinning) require sophisticated equipment and parameter settings, while rarely including natural components or relying on homogeneous solutions.

The approach presented in this dissertation is based on the use of homogeneous solutions containing PEO, a biodegradable aliphatic polyester (PLA, PCL, PBS, PLAGA or PHB), and beeswax (BW) - as an entirely new method for producing fibers with a self-organized core-sheath architecture, without the need for a coaxial nozzle.

The incorporation of biologically active compounds such as 5-nitro-8-hydroxyquinoline (NQ) and 5-chloro-7-iodo-8-hydroxyquinoline (CQ) enables direct applications of these fibers as pharmaceutical dosage forms with prolonged release, wound dressings with antibacterial and anticancer effects, as well as potential systems for targeted therapy.

In addition, the inclusion of beeswax - a natural component with pronounced antioxidant and barrier properties; imparts a unique profile to the fibers: a hydrophobic surface with stable morphology even upon contact with water, which is atypical for systems containing PEO.

This ternary combination of a synthetic, biodegradable, and natural component, coupled with self-organization during electrospinning, represents a fundamental scientific contribution, opening a new pathway for the development of multifunctional

fibers with potential applications across interdisciplinary domains, ranging from oncology to environmentally sustainable materials.

II. GOALS AND OBJECTIVES OF THE DISSERTATION WORK

The aim of the dissertation has been to establish suitable conditions for the preparation of composite fibers with core–sheath architecture by electrospinning of homogeneous solutions of PEO/BW or PEO/polyester/BW without the use of an auxiliary device for coaxial electrospinning. The possibility of employing these materials as carriers of model bioactive agents has been studied in order to obtain a new type of non-woven textile with antibacterial, antifungal, and anticancer activity.

In order to achieve this aim, the following objectives were set:

1. To obtain fibers with core-sheath architecture from PEO/BW by electrospinning of homogeneous solutions of the partners.
2. To obtain fibers with core-double sheath architecture from PEO/PLA/BW by electrospinning of homogeneous solutions of the partners.
3. To prove the validity of the proposed approach for producing fibers with "core-double sheath" architecture by replacing PLA with another biodegradable aliphatic polyester, such as PCL, PLAGA, PBS, or PHB. To investigate the effect of the ratio of molecular weights of PEO and the polyester on the composition of the core, inner, and outer sheath of the fibers.
4. To assess the antibacterial, antifungal, and anticancer activity of the new fibrous materials loaded with NQ or CQ.

III. RESULTS AND DISCUSSION

Chapter 1. Fibers with "core-sheath" architecture from PEO and BW obtained by electrospinning of homogeneous solutions of the partners. .^{[P1], [OP1,OP2, OP3], [PP1,PP2]}

For the first time, composite fibrous materials from PEO and BW were obtained by electrospinning of homogeneous solutions of the partners in their common solvent chloroform. The resulting PEO/BW fibers exhibited a "core-sheath" architecture, as confirmed by water contact angle measurements, surface elemental composition analysis, and selective extraction of PEO and BW in water and hexane, respectively. In addition, the core-sheath structure was demonstrated by TEM. It was shown that, due to the good solubility of the model drug NQ in chloroform, it could be incorporated in a single step into PEO/BW fibrous materials by electrospinning, and the resulting fibers also exhibited a core-sheath architecture.

1.1. Composite fibrous materials from PEO/BW obtained at different weight ratios of the partners

Composite fibrous materials from PEO/BW were obtained by electrospinning of their solutions in chloroform at weight ratios PEO/BW = 90/10, 80/20, 70/30, 60/40, and 50/50. The corresponding mats are denoted as: PEO(80)/BW(20), PEO(70)/BW(30), PEO(60)/BW(40), and PEO(50)/BW(50). SEM micrographs of the respective fibrous materials are presented in **Figure G1-1**. As can be seen, at BW content up to 30 wt.%, the fibers are cylindrical and defect-free. At a weight ratio of PEO(60)/BW(40) (**Figure G1-1G**), in addition to cylindrical fibers, areas where the fibers are stacked together were observed, as well. The tendency for the fibers to stick together was even more pronounced in mats from PEO(50)/BW(50) (**Figure G1-1D**). **Figure G1-1E** presents the dependence of the mean diameter of PEO/BW fibers on BW content. The lowest mean fiber diameters were observed for mats obtained at PEO(80)/BW(20) and PEO(70)/BW(30).

The thermal behavior of the new fibrous materials was investigated by DSC. The presence of BW led to broadening of the melting peak of PEO at around 65 °C (**Figure G1-2** in the dissertation).

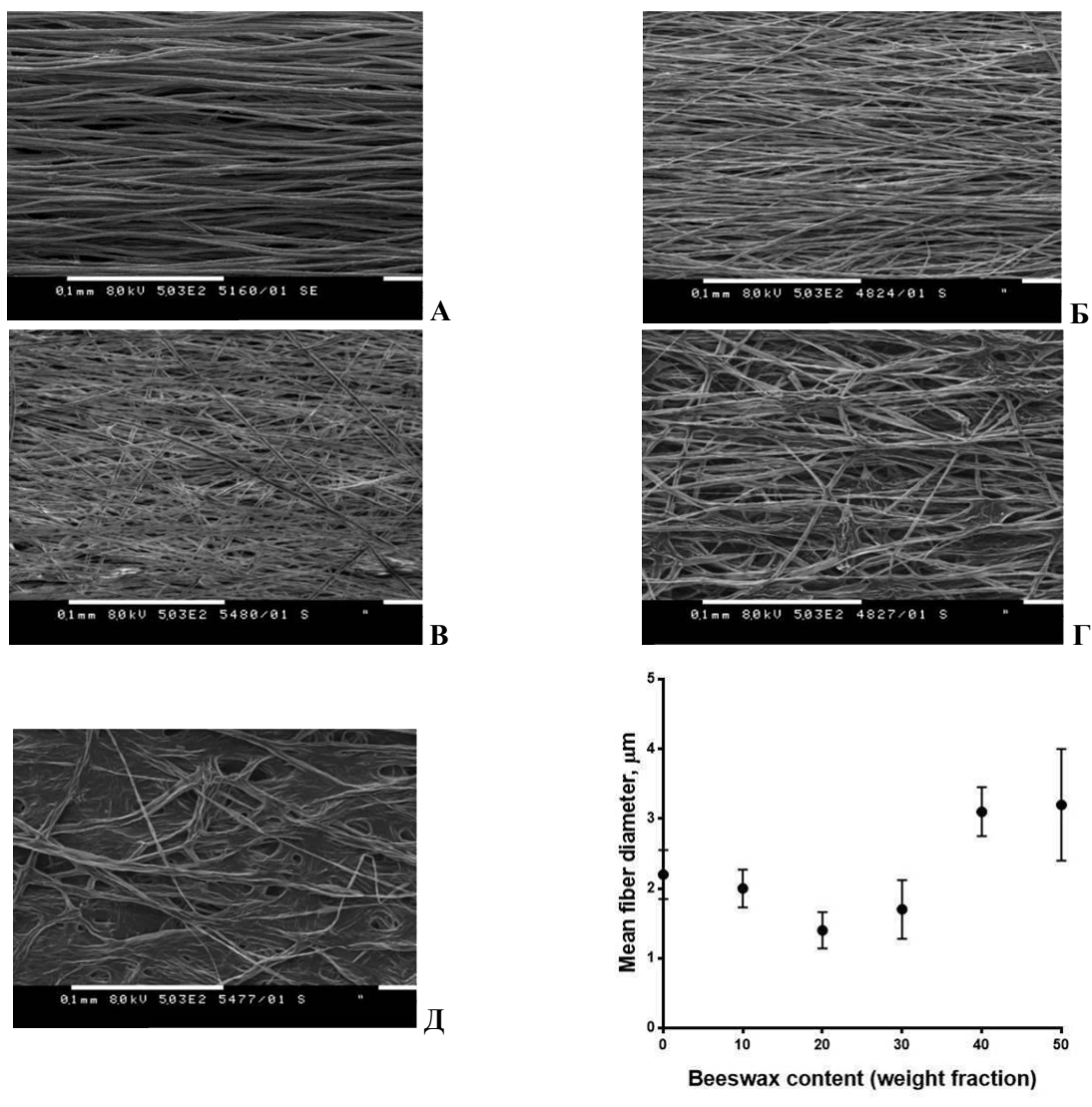


Figure G1-1. SEM micrographs of fibrous materials from PEO/BW obtained at weight ratios: PEO(90)/BW(10) (A), PEO(80)/BW(20) (B), PEO(70)/BW(30) (C), PEO(60)/BW(40) (D), and PEO(50)/BW(50) (E). Magnification: $\times 500$. Dependence of the average fiber diameter of PEO/BW on wax content in the spinning solution (F).

The amorphous/crystalline characteristics of the fibrous materials were also evaluated by X-ray diffraction (XRD). The mats exhibited crystalline phases originating from both the polymer and BW (Figure G1-3 in the dissertation). With increasing BW content in the PEO/BW mats, the diffraction intensities at 19.2° and 23.3° , characteristic of the crystalline phase of PEO, decreased, whereas the intensity of the diffraction peak at 21° , characteristic of the crystalline phase of BW, increased.

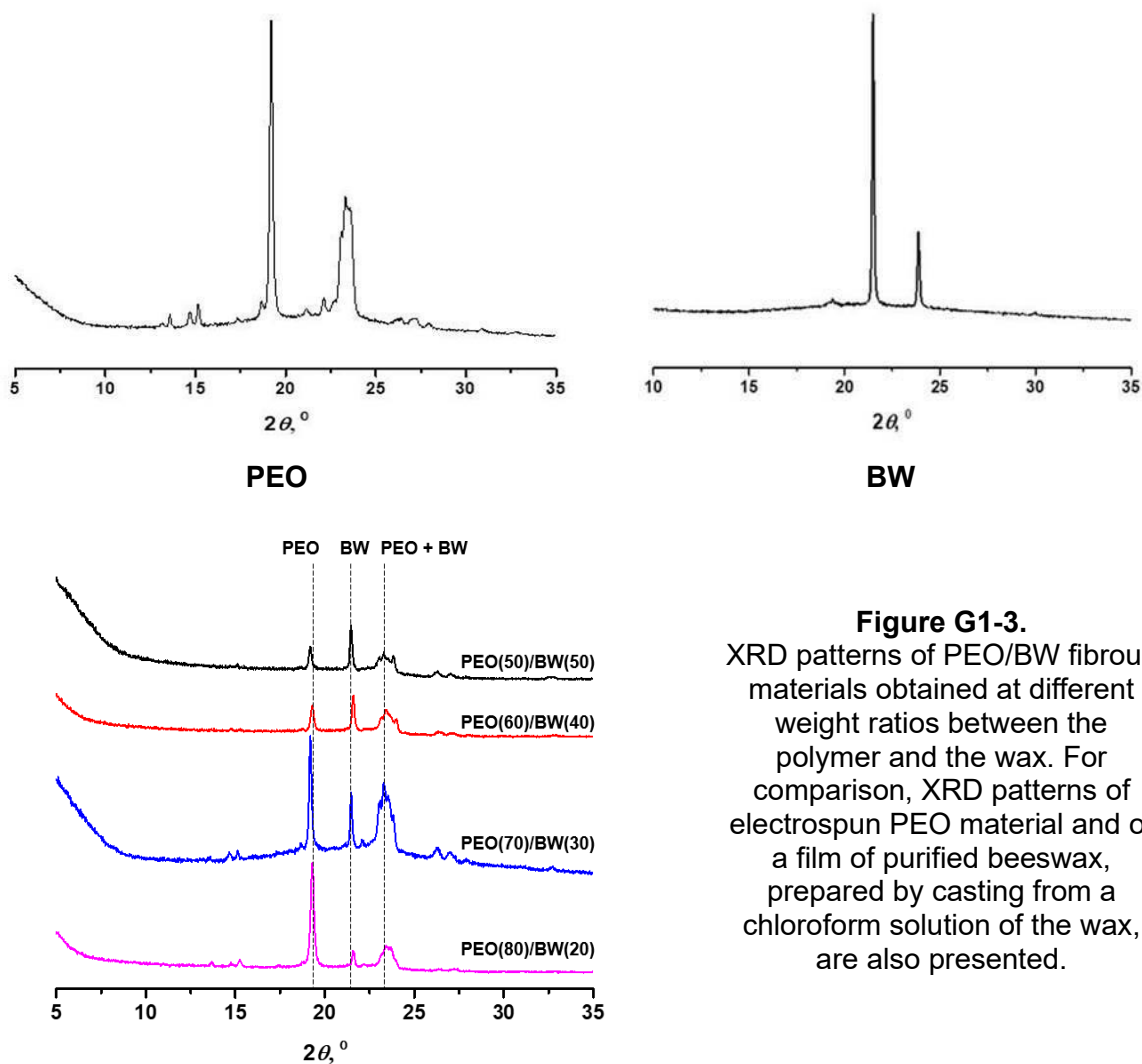


Figure G1-3. XRD patterns of PEO/BW fibrous materials obtained at different weight ratios between the polymer and the wax. For comparison, XRD patterns of electrospun PEO material and of a film of purified beeswax, prepared by casting from a chloroform solution of the wax, are also presented.

The effect of BW incorporation on the hydrophilic/hydrophobic surface characteristics of the electrospun PEO/BW materials was investigated by determining the water contact angle. It was found that, unlike the PEO mat, which is hydrophilic, the PEO/BW fibrous materials are hydrophobic, exhibiting a water contact angle greater than 100°. To explain the surface hydrophobization of the PEO-based fibrous materials and the unexpectedly high water contact angle, the chemical composition of the mat surfaces was examined. The latter was quantitatively assessed by XPS. In the detailed C1s spectrum of a PEO fibrous material, only a single peak was detected at 286.45 eV, characteristic of a carbon atom involved in an ether bond in the polymer macromolecule (**Figure G1-5**).

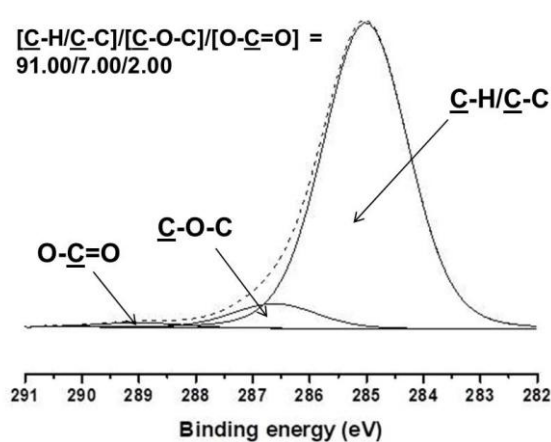
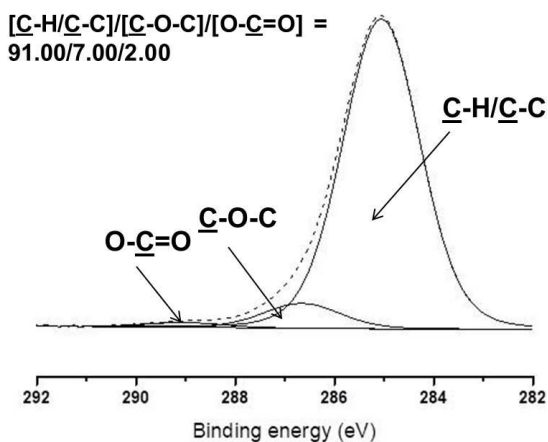
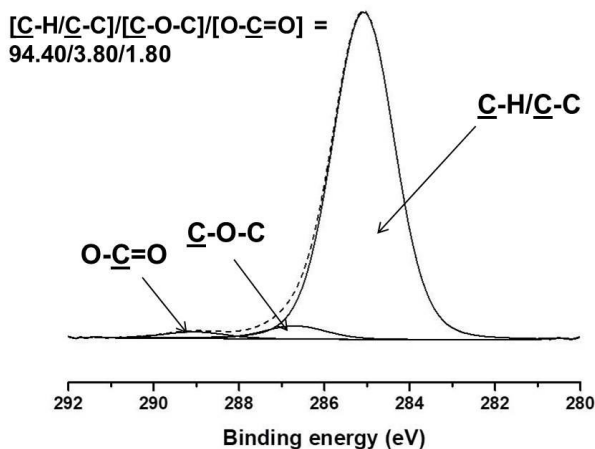
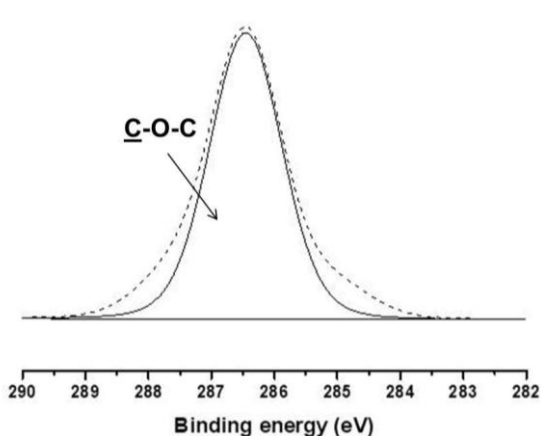


Figure G1-5. Detailed C 1s spectra of a PEO mat and of BW, as well as of PEO(70)/BW(30) and PEO(50)/BW(50) mats.

The detailed C1s spectrum of BW is more complex, displaying three peaks at 285.08, 286.68, and 289.05 eV, corresponding to carbon atoms involved in C–C/C–H, ether, and carbonyl groups, respectively. As shown in **Figure G1-5**, the C1s spectra of the PEO/BW mats exhibit a similar pattern to that of the wax, again revealing three peaks characteristic of carbon atoms involved in C–C/C–H, ether, and carbonyl groups. Notably, the determined ratio of the three types of carbon atoms $[C-H/C-C]/[C-O-C]/[O-C=O] = 91.00/7.00/2.00$ in the PEO/BW mats is close to that of BW (**Figure G1-5**). This provides further evidence that wax is present on the surface of these fibers.

The results of the TEM analyses of the electrospun PEO/BW materials confirm that the fibers possess a core-sheath structure, with a core composed of PEO and a sheath - of BW (**Figure G1-6**).

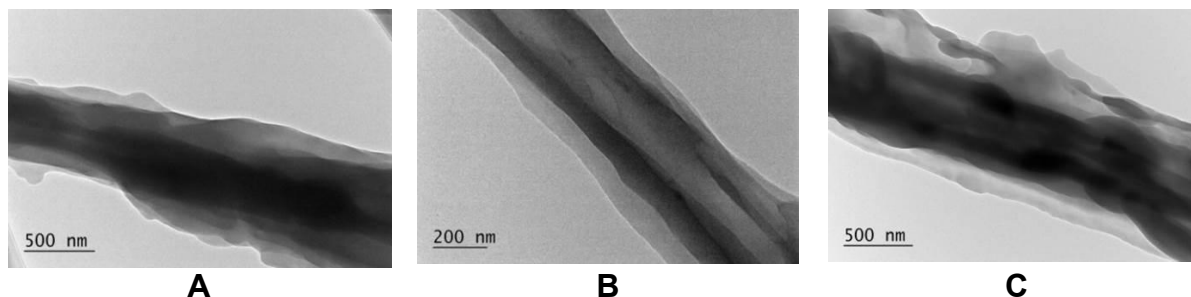


Figure G1-6. TEM micrographs of a single fiber from: PEO(80)/BW(20) (A), PEO(70)/BW(30) (B), and PEO(60)/BW(40) (C). Magnification: $\times 10,000$ (A and C) or $\times 20,000$ (B).

1.2. Electrospun composite fibrous materials of PEO/BW containing NQ

5-Nitro-8-hydroxyquinoline (NQ) was incorporated into the electrospinning system as a model bioactive compound due to its antimicrobial and anticancer properties. The determined loading efficiency of NQ in the mats was $98 \pm 1.0\%$. SEM analyses revealed that the presence of NQ in the spinning solution did not significantly alter the mean fiber diameter, but resulted in the formation of thin fibrous branches along the main fibers, which diminished their length with increasing BW content (**Figure G1-7** in the dissertation). XRD analyses showed that NQ is present in an amorphous state in the fibrous materials with high PEO content (PEO(80)/BW(20)/NQ) and in a crystalline state in materials with higher BW content (PEO(60)/BW(40)/NQ) (**Figure G1-8** in the dissertation). On the surface of PEO(70)/BW(30)/NQ and PEO(60)/BW(40)/NQ mats, the presence of NQ was confirmed by the detailed N1s spectra of nitrogen atoms obtained by XPS (**Figure G1-9** in the dissertation).

Due to the hydrophobic surface characteristics of the electrospun materials and the presence of air-filled voids in their structure, they do not sink when placed in an aqueous medium but remain floating on its surface. This complicates the acquisition of reliable results in drug release studies. Therefore, a special cell was designed that allows the investigated fibrous material to be fully immersed in the aqueous medium (**Figure OC-2** in the dissertation). The amount of NQ released over time was found not to depend significantly on the weight ratio between PEO and BW (**Figure G1-10** in the

dissertation). The weight loss of the mats after incubation in buffer solution (pH 7.4, ionic strength 0.1) was also determined. The results showed that after 24 h in the aqueous medium, PEO and NQ had dissolved and leached out from the fibrous mat structure. SEM observation of the fragments obtained after 24 h of incubation of a PEO(80)/BW(20)/NQ mat in buffer solution revealed structures resembling fibers cut longitudinally, which led us to assume that these fragments represented BW sheaths which structure was disrupted due to the swelling and dissolution of the PEO core.

To further confirm the core–sheath structure, an extraction experiment was carried out using hexane as a solvent, which does not dissolve PEO and NQ but dissolves BW very well. It was found that after 24 h of immersion of the fibrous materials in hexane, the mats did not fragment and, after drying, they were not brittle but retained their flexibility, indicating that they were composed of PEO. In addition, the extraction with hexane led to a decrease in the average fiber diameter, which we attributed to the dissolution of the wax. After immersion of the mats in hexane and subsequent drying in air at room temperature, they were placed in distilled water. A rapid dissolution of the mat was observed, suggesting that after hexane treatment the entire amount of BW was extracted from the PEO/BW/NQ mats. This provides further evidence for the presence of a structure consisting of a PEO core and a BW sheath (**Scheme G1-2** in the dissertation).

An original approach has been proposed to prepare fibers with a core-sheath architecture from PEO/BW and PEO/BW/NQ, consisting of a PEO core and a BW shell, by electrospinning of homogeneous blend solutions of the components without the use of an auxiliary coaxial electrospinning device. This effect is attributed to the self-organization of BW molecules on the fiber surface during the electrospinning process, driven by the incompatibility between PEO and BW as well as by the hydrophobicity of air. In addition, the difference between the molecular weight of PEO and the molecular weights of the constituents of BW also plays a role. As a mixture of substances with lower molecular weight compared to PEO, BW exhibits greater mobility during the fiber formation by electrospinning and thus forms the sheath of the fiber, while PEO is responsible for the formation of the fiber core. The newly obtained fibrous materials are of interest as carriers of bioactive compounds.

Chapter 2. Fibers with a core-double sheath architecture of PEO, PLA, and BW obtained by electrospinning of homogeneous solutions of the components . [P2], [OP2], [PP2]

At the next stage of the study, the biocompatible and biodegradable aliphatic polyester poly(L-lactide) (PLA) with a molar mass of 259 000 g/mol (lower than that of PEO and higher than that of the components in BW) was added to the the spinning solution of PEO (molar mass of 600 000 g/mol) and BW. The aim was to investigate the effect of PLA on the fiber architecture. For the first time, composite PEO/PLA/BW fibers with a core-double sheath structure were obtained by single-nozzle spinneret electrospinning. The architecture was confirmed by TEM, XPS, and selective extraction with an appropriate solvent. It was evidenced that the fibers consisted of a PEO core, a PLA inner sheath, and a BW outer sheath. Mats composed of these fibers exhibited significantly improved mechanical properties compared to mats from PEO, PLA, or PEO/BW. This represents the first report on the preparation of composite fibers with a core-double sheath architecture through electrospinning of homogeneous solutions of the components using a single-nozzle spinneret. A model drug NQ was successfully incorporated into the spinning solution, indicating that such mats may be applied as carriers of bioactive substances.

2.1. Composite fibrous materials of PEO/PLA/BW obtained at different weight ratios of the components

Fibrous materials of PEO/PLA/BW were obtained at weight ratios of PEO/PLA/BW = 80/10/10, 70/15/15, 60/20/20, and 50/25/25 using chloroform as a common solvent. The corresponding mats are hereafter designated as PEO(80)/PLA(10)/BW(10), PEO(70)/PLA(15)/BW(15), PEO(60)/PLA(20)/BW(20), and PEO(50)/PLA(25)/BW(25) (SEM micrographs and the mean diameters of the resulting fibers are presented in **Figure G2-1** and **Figure G2-2** of the dissertation, respectively). It was found that the fibrous materials of PEO(80)/PLA(10)/BW(10) are hydrophobic, with a water contact angle of $101 \pm 8.85^\circ$. A further increase in the content of PLA and BW did not result in a significant increase in the water contact angle (remaining ca. 118°). In conclusion, the presence of the hydrophobic PLA and BW in the electrospun solutions imparts hydrophobicity to the surfaces of the PEO/PLA/BW mats.

Figure G2-3 presents TEM micrographs of the newly obtained fibrous materials. As can be seen, they exhibit a core–double sheath structure, with the core composed of PEO ($\bar{M}_n = 600\,000$ g/mol), the inner shell of PLA ($\bar{M}_w = 259\,000$ g/mol), and the outer sheath of BW. Based on the TEM micrographs, the areas of segments from the core and the two sheaths were calculated, as well as the ratio of the sheath area to the core area (**Table G2-1** in the dissertation). It was found that with increasing PLA and BW content, the sheath-to-core ratio increased from 0.24 to 0.63, indicating that higher amounts of PLA and BW led to the formation of fibers with thicker sheaths.

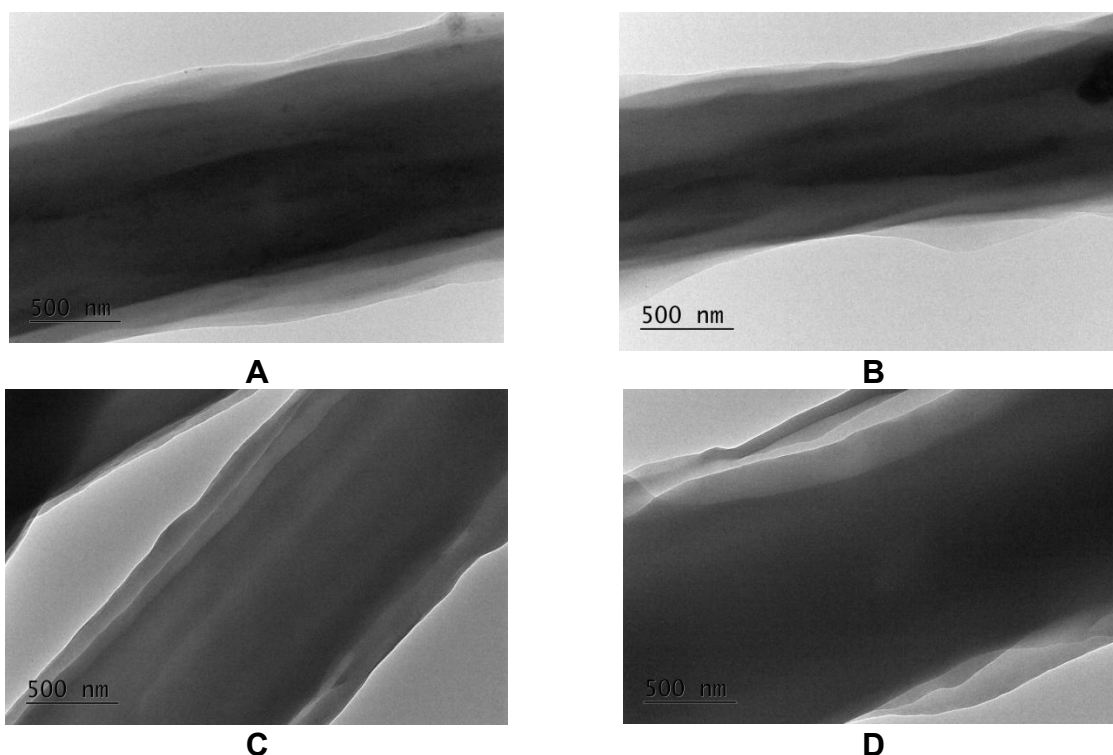


Figure G2-3. TEM micrographs of a fiber from: PEO(80)/PLA(10)/BW(10) (A), PEO(70)/PLA(15)/BW(15) (B), PEO(60)/PLA(20)/BW(20) (C), and PEO(50)/PLA(25)/BW(25) (D); magnification: $\times 10,000$.

To confirm the architecture of the PEO/PLA/BW fibers, selective extraction of BW in hexane and of PEO in water was carried out. The weight loss of the mats after 24 hours of immersion in hexane was determined and compared with the theoretical weight loss, calculated under the assumption that the entire amount of BW had been extracted from the mats into hexane (**Figure G2-4** in the dissertation). It was found that the experimentally determined weight loss was equal to the theoretical value, indicating that 24 h of immersion in hexane is sufficient for the almost complete extraction of BW from

the fibrous materials. SEM analyses showed that the mean fiber diameter of mats composed of PEO(60)/PLA(20)/BW(20) or PEO(50)/PLA(25)/BW(25) changed only slightly after 24 h of immersion in hexane (**Figure G2-5**). TEM micrographs of single fibers revealed that, after hexane extraction, the fibers consisted of a core and a single sheath. The ratio of the sheath area to the core area was also determined, and it was found to be lower than that measured for the initial fibers (**Table G2-1** in the dissertation). Additional evidence that the fibers were composed of a PEO core and a single PLA sheath was obtained by determining the water contact angle of the hexane-treated mats. It was found that they remained hydrophobic, with a water contact angle of approximately $109 \pm 7^\circ$.

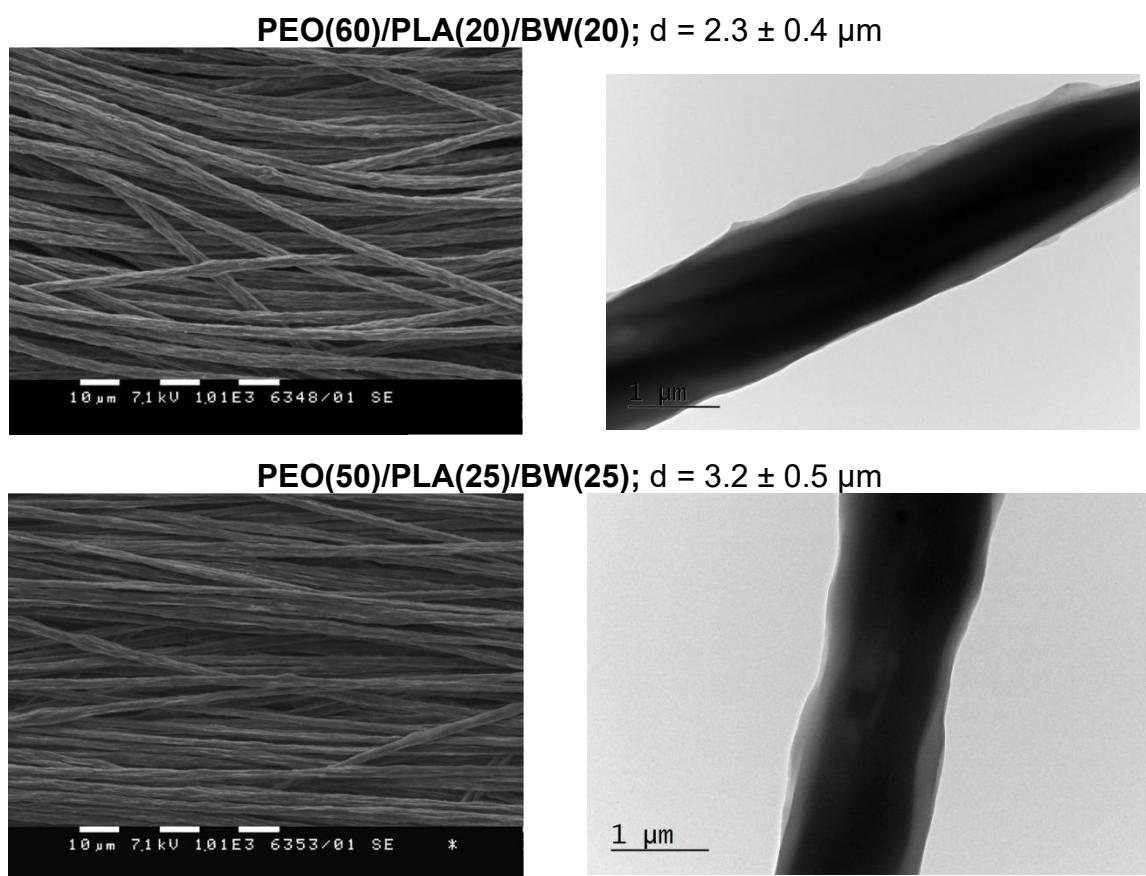


Figure G2-5. SEM micrographs of mats and TEM micrographs of single fibers from PEO(60)/PLA(20)/BW(20) and PEO(50)/PLA(25)/BW(25) mats after 24 h of immersion in hexane.

In the next stage, hexane-treated mats of PEO(60)/PLA(20)/BW(20) were immersed in distilled water for 48 h. It was found that, due to the swelling and leaching of PEO from

the fibers, immersion of the mat in distilled water resulted in fiber sticking (**Figure G2-6A** in the dissertation).

The FTIR spectra of BW pellets, a PLA mat, a PEO mat, and a PEO(60)/PLA(20)/BW(20) mat were compared before and after extraction with hexane (24 h), as well as after sequential treatment with hexane (24 h) and water (48 h) (**Figure G2-7** in the dissertation). It was found that hexane extraction led to the dissolution of BW from the PEO(60)/PLA(20)/BW(20) mats, as evidenced by the absence of the characteristic bands of methyl and methylene groups of the wax in the 3000–2800 cm^{-1} region, as well as the absence of the shoulder at 1735 cm^{-1} corresponding to the carbonyl group of the carboxyl groups in fatty acids. Subsequent water extraction resulted in the removal of PEO, indicated by the absence of the characteristic absorption bands of the CH_2 groups of PEO in the 3000–2800 cm^{-1} region.

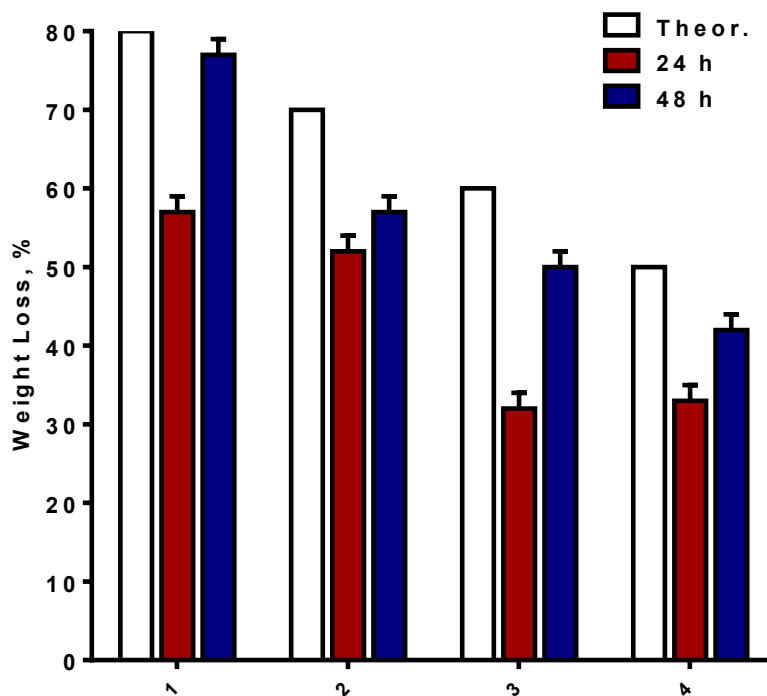


Figure G2-8. Dependence of the weight loss of mats from the PEO/PLA/BW series, obtained at weight ratios of PEO(80)/PLA(10)/BW(10) (1), PEO(70)/PLA(15)/BW(15) (2), PEO(60)/PLA(20)/BW(20) (3), and PEO(50)/PLA(25)/BW(25) (4), on the composition of the fibrous materials after 24 and 48 h of immersion in distilled water. For comparison, the theoretical weight loss is also presented, calculated under the assumption that the entire amount of PEO was extracted from the respective mats after immersion in water.

The weight loss of the fibrous materials from the PEO/PLA/BW series was also determined after contact with distilled water, depending on the immersion time of the mats, namely 24 and 48 h (**Figure G2-8**). It was found that 24 h of immersion in water was not sufficient for the complete extraction of PEO. For comparison, in the case of PEO/BW mats discussed in Chapter 1, the gravimetric analysis showed that the entire amount of PEO leached out from the fibrous materials after 24 h-stay in an aqueous medium. This provides evidence that the presence of a second, inner PLA sheath in the PEO/PLA/BW fibers delays the release of PEO from the fiber core. The experimentally determined weight loss of the PEO/PLA/BW mats approached the theoretical value after 48 h of immersion in distilled water, indicating that within this period of time nearly all PEO was released into the aqueous medium.

The surface chemical composition of the PEO/PLA/BW fibrous materials was evaluated by XPS. It was found that the surface composition of the PEO/PLA/BW fibers closely resembled that of BW (**Figure G2-10** in the dissertation). This led to the conclusion that the outermost sheath of the core–double sheath fibers is composed of BW.

The thermal characteristics of the PEO/PLA/BW fibrous materials were assessed by DSC. The DSC thermograms exhibited two melting peaks at approximately 65 °C and 166 °C (**Figure G2-11**). The first peak corresponds to the melting of PEO and BW; their melting in a similar temperature range makes it difficult to distinguish them. The second peak at 166 °C is attributed to the melting of PLA in the composite fibrous materials. Using the enthalpy of melting of PLA, the degree of crystallinity of the aliphatic polyester in the composite fibers was determined (close to 50%), taking into account its weight fraction in the mat (**Figure G2-11** and **Table G2-2** in the dissertation). The amorphous/crystalline structure of the PEO/PLA/BW fibrous materials was evaluated by XRD. The XRD patterns of the fibrous materials showed crystalline phases of the all three components (**Figure G2-12** in the dissertation). Additional evidence for the removal of BW from the fibrous materials after hexane extraction was obtained from the XRD patterns of fibers after 24 h of immersion in hexane, where the reflection at 21°, characteristic of BW, was absent (**Figure G2-13** in the dissertation).

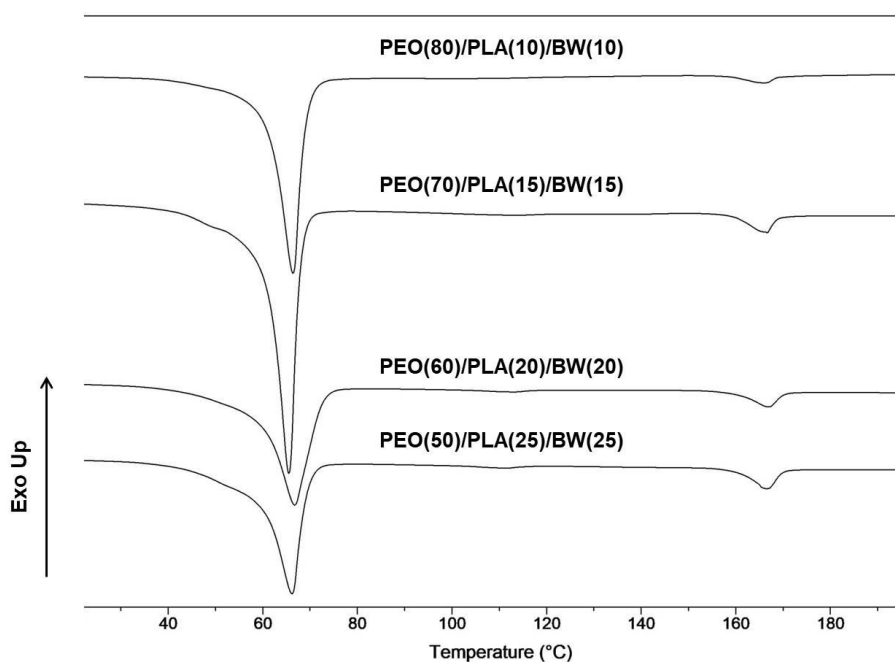


Figure G2-11. DSC thermograms (first heating run) of PEO/PLA/BW fibrous materials obtained at different weight ratios of the components, recorded using a Discovery DSC 250 differential scanning calorimeter (TA Instruments, USA).

Figure G2-14 presents the stress–strain curves of fibrous materials of PEO, PLA, and PEO/PLA/BW. It was found that the PEO/PLA/BW mats (**Figure G2-14B**) exhibited significantly improved mechanical properties compared to fibrous materials of PEO and PLA (**Figure G2-14A**), as well as to PEO/BW mats. In PEO/PLA/BW mats obtained at weight ratios of 80/10/10, 70/15/15, or 60/20/20, necking was observed, with the specimens undergoing significant elongation (**Figure G2-14B**) and not breaking even after 200% extension. The tensile strength (σ) and Young’s modulus (E) increased with increasing PLA content, reaching values close to 5.5 MPa and 425 MPa, respectively, in PEO(60)/PLA(20)/BW(20). This can be attributed to the higher content of PLA, which is the component exerting a positive effect on these two parameters. The high elasticity of these fibrous materials was attributed to the presence of PEO in the mats. In PEO(50)/PLA(25)/BW(25), the values of σ and E were lower, and the brittleness higher, due to the high BW content. To further demonstrate the contribution of PLA to the improved mechanical properties of PEO/PLA/BW fibrous materials, the mechanical

properties of a PEO(70)/BW(30) mat were compared with those of a mat in which 15% of BW was replaced with PLA, namely PEO(70)/PLA(15)/BW(15).

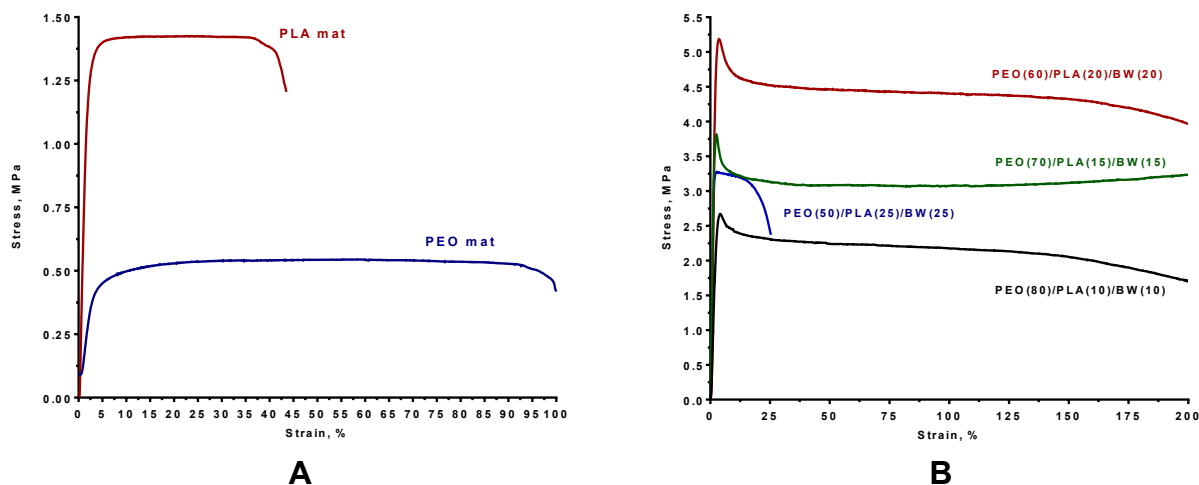


Figure G2-14. Stress–strain curves recorded during the tensile test of electrospun samples of PEO or PLA (A) and of the PEO/PLA/BW series (B).

It was found that the PEO(70)/BW(30) mat exhibited lower mechanical performance compared to the PEO(70)/PLA(15)/BW(15) mat, namely: a tensile strength (σ) of 0.40 ± 0.04 MPa [while the σ value of the PEO(70)/PLA(15)/BW(15) mat was close to 4 MPa], a Young’s modulus (E) of 18 ± 2 MPa [compared to approximately 350 MPa for the PEO(70)/PLA(15)/BW(15) mat], and an elongation at maximum load (ϵ) of about 53% [whereas the ϵ value of the PEO(70)/PLA(15)/BW(15) mat exceeded 200%]. In the PEO(70)/BW(30) mats, the specimens fractured upon reaching their maximum elongation. Therefore, the presence of PLA in the mats is the reason for the significant improvement of the mechanical properties of the PEO/BW-based fibrous materials.

2.2. Composite fibrous materials of PEO/PLA/BW/NQ

To demonstrate the potential of the new fibrous materials as drug carriers, NQ was used as a model drug compound with pronounced antibacterial and antifungal activity. Mats were obtained at different weight ratios of PEO/PLA/BW, in which the NQ content was 10 wt.% relative to the total dry mass. It was established that the presence of NQ did not cause significant alterations in the mean fiber diameters values. However, similar to the PEO/BW/NQ system, thin fibrous whiskers were observed, with diameters of about 600 nm, which did not depend on the PEO/PLA/BW ratio (Figure G2-17 in the dissertation).

TEM analyses (**Figure G2-18**) demonstrated that the presence of NQ did not disrupt the formation of the core-double sheath structure. XPS analyses showed that in PEO/PLA/BW/NQ mats, BW was present on the fiber surface. Only traces of NQ were detected on the fiber surface, with its amount not exceeding 1%. The incorporation of NQ also did not affect the hydrophilic/hydrophobic characteristics of the materials, which remained hydrophobic, with a water contact angle of $115 \pm 5.86^\circ$ (**Figure G2-19** in the dissertation).

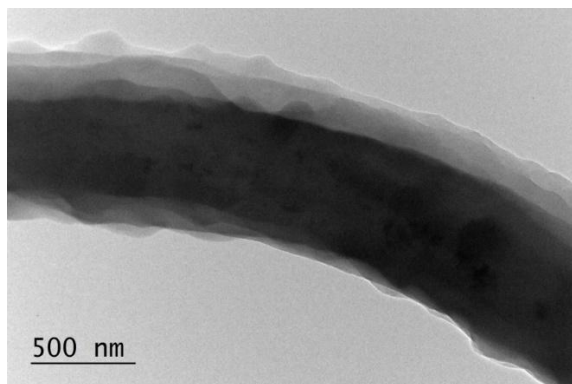


Figure G2-18. TEM micrograph of a fiber from PEO(50)/PLA(25)/BW(25)/NQ.

XRD analyses showed that the most intense diffractions of NQ in the 2θ range of $10\text{--}15^\circ$ were difficult to be distinguished in XRD patterns of the PEO/PLA/BW/NQ mats, since they fell within the detected amorphous halo of PLA (**Figure G2-20** in the dissertation). DSC analyses revealed that the degree of crystallinity of PLA incorporated in the fibrous materials was about 35% (**Figure G2-21** in the dissertation). A melting peak for NQ at around 180°C was observed only in the PEO(50)/PLA(25)/BW(25)/NQ mat. In the other mats, no melting peak for NQ was registered, indicating that in these materials the drug is in an amorphous state. The presence of NQ did not significantly affect the elongation at break of the materials (**Figure G2-22** in the dissertation). The release of NQ from the mats was monitored spectrophotometrically using a phosphate buffer solution (pH 7.4, ionic strength 0.1). It was found that the composition of the fibrous carrier did not have a significant influence on the amount of NQ released over time (**Figure G2-23** in the dissertation).

For the first time, fibers with core-double sheath architecture were obtained by electrospinning of homogeneous solutions of the components using a single-nozzle spinneret. This was achieved by electrospinning of homogeneous solutions of PEO,

PLA, and BW. It was demonstrated that the core-double sheath fibers of the PEO/PLA/BW system consist of a PEO core, a PLA inner sheath, and a BW outer sheath. This was attributed to the differences in the molar masses of the components and, consequently, to their different abilities to migrate toward the surface of the spinning jet during the electrospinning and thus toward the surface of the forming fiber. BW, as a mixture of low-molecular-weight substances, is characterized by the highest mobility and therefore forms the outer sheath of the fiber. PLA with an intermediate molar mass exhibits lower mobility compared to BW but higher mobility than PEO, resulting in the formation of the inner sheath of the fiber. PEO, being the component with the highest molar mass, forms the fiber core. In addition, the incompatibility of the components as well as the hydrophobicity of air also contribute to the formation of PEO/PLA/BW fibers with a core-double sheath architecture. Furthermore, it was demonstrated that non-woven textiles composed of PEO/PLA/BW fibers could serve as carriers of bioactive agents.

Chapter 3. Validation of the proposed approach for obtaining fibers with a core–double sheath architecture by replacing PLA with another biodegradable aliphatic polyester, such as PCL, PLAGA, PBS, or PHB. Evaluation of the effect of the molar mass ratio of PEO and the polyester on the composition of the core, the inner sheath, and the outer sheath of the fibers. ^[P3,P4] ^[OP2, OP3]

It was of particular interest to validate the approach proposed in Chapter 2 for obtaining fibers with a core-double sheath architecture by replacing PLA with another biocompatible and biodegradable polyester such as PCL, PLAGA, PBS, or PHB. The single-nozzle spinneret electrospinning of homogeneous PEO/polyester/BW solutions resulted in fibers with a core-double sheath structure. The influence of the molar mass ratio of PEO and the polyester on the composition of the inner sheath and the core of the fibers was also assessed. It was found that when the molar mass of the polyester is lower than that of PEO, fibers with a well-defined PEO core, a polyester inner sheath, and a BW outer sheath were formed. In contrast, when the polyester had a higher molar mass than PEO, the polyester macromolecules were detected in the PEO core, and PEO chains were present in the polyester inner sheath. For the first time, sequential selective extraction of the outer and inner sheath was applied using hexane and THF, respectively, as solvents. It was found that the mechanical characteristics of

PEO/polyester/BW fibrous materials depended on the polyester nature. Furthermore, the possibility of targeted deposition of hydrophilic or hydrophobic substances in the core or the sheaths of PEO/polyester/BW fibers was demonstrated, using nanosized zinc oxide with either an unmodified (hydrophilic) or silanized (hydrophobic) surface as a contrast agent. Finally, it was shown that the release of NQ incorporated in PEO/BW, PEO/PCL/BW, and PEO/PLA/BW fibers during the initial release stages depended on both the fiber architecture and the nature of the polyester.

3.1. Composite fibers with a core–double sheath architecture of PEO/polyester/BW obtained by electrospinning of homogeneous solutions of the components

In Chapter 3, the following polymers were used: PEO with a molar mass of 600 000 g/mol, PEO with a molar mass of 100,000 g/mol, poly(L-lactide) with a molar mass of 259 000 g/mol, and poly(L-lactide-co-D,L-lactide) with a molar mass of 911 000 g/mol. These were designated as PEO600k, PEO100k, PLA259k, and PLA911k, respectively.

3.1.1. Core-double sheath fibers obtained using a polyester with a molar mass lower than that of PEO

Electrospinning of homogeneous solutions of PEO600k and polyesters such as PCL (molar mass 69 000 g/mol), PLAGA (molar mass 76 000 – 115 000 g/mol), PBS (molar mass 97 600 g/mol), PLA259k, and PHB (molar mass 330 000 g/mol) at a ratio of PEO/polyester/BW = 60/20/20 (w/w/w) resulted in fibers oriented in the direction of the collector rotation (**Figure G3-1** in the dissertation). The PEO/PCL/BW fibers had the smallest diameter ($1.80 \pm 0.25 \mu\text{m}$), which was attributed to the lowest molar mass of PCL (69 000 g/mol). The use of polyesters with higher molar mass led to the formation of fibers with larger diameters. TEM micrographs (**Figure G3-2** in the dissertation) clearly showed the core-double sheath structure. The formation of this structure is due to phase separation arising from the incompatibility of the components and their molar mass differences. Thus, PEO forms the core, the polyester forms the inner sheath, and BW, being the lowest molar mass and the most mobile component, distributes along the fiber surface during the solvent evaporation in the electrospinning process. The water contact angle of all investigated fibrous materials exceeded 110° , confirming that the surface is composed of the hydrophobic components - BW and the polyester.

To confirm the core-double sheath structure, for the first time a systematic approach was applied, consisting of sequential selective extraction with hexane and THF (**Scheme G3-1** in the dissertation). After hexane extraction, it was found that the experimentally determined weight loss was close to the theoretically calculated value, indicating almost complete removal of BW from all studied fibrous materials (**Figure G3-3** in the dissertation). Additional evidence was the observed decrease in the fiber diameter and the transition from a core-double sheath structure to a core-sheath structure (**Figures G3-4** and **G3-6** in the dissertation). The fibers retained their hydrophobic behavior, with a measured water contact angle of about 110° , which is indicative for the presence of a remaining hydrophobic polyester inner sheath. FTIR analysis further confirmed the removal of BW by the disappearance of the characteristic stretching vibrations of CH_2 and CH_3 groups of the wax at 2915 and 2848 cm^{-1} (**Figures G3-5** and **G3-7** in the dissertation).

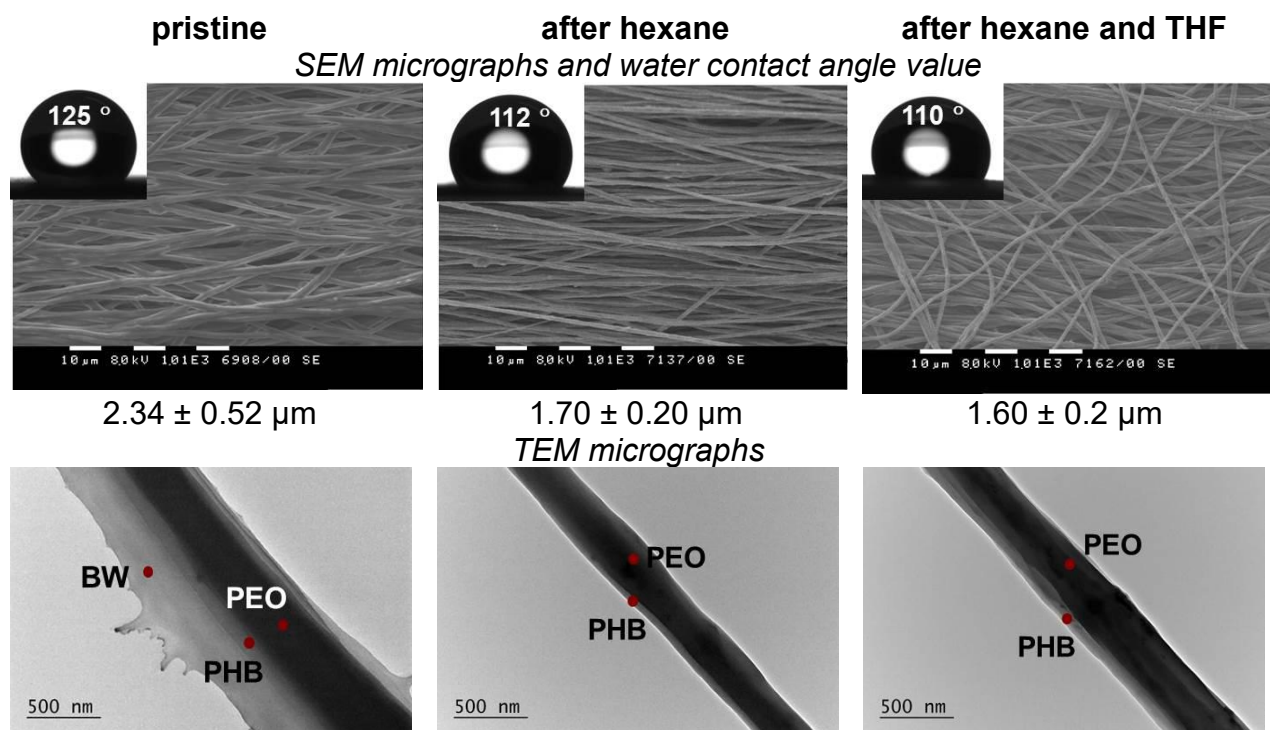


Figure G3-4. SEM and TEM micrographs of a mat and of single fibers from PEO/PHB/BW before and after sequential selective extraction with hexane and THF. The mean fiber diameters determined from the SEM micrographs are indicated. The measured water contact angles before and after sequential selective extraction with hexane and THF are also shown. Magnification of SEM micrographs: $\times 1,000$; magnification of TEM micrographs: $\times 10,000$.

Subsequent treatment with THF yielded results that depended on the solubility of the polyester used. In mats containing polyesters insoluble in THF, such as PHB and PBS, the weight loss was significantly lower than the theoretical value (7% and 2%, respectively), and the fibers retained their hydrophobicity (**Figure 3-4**).

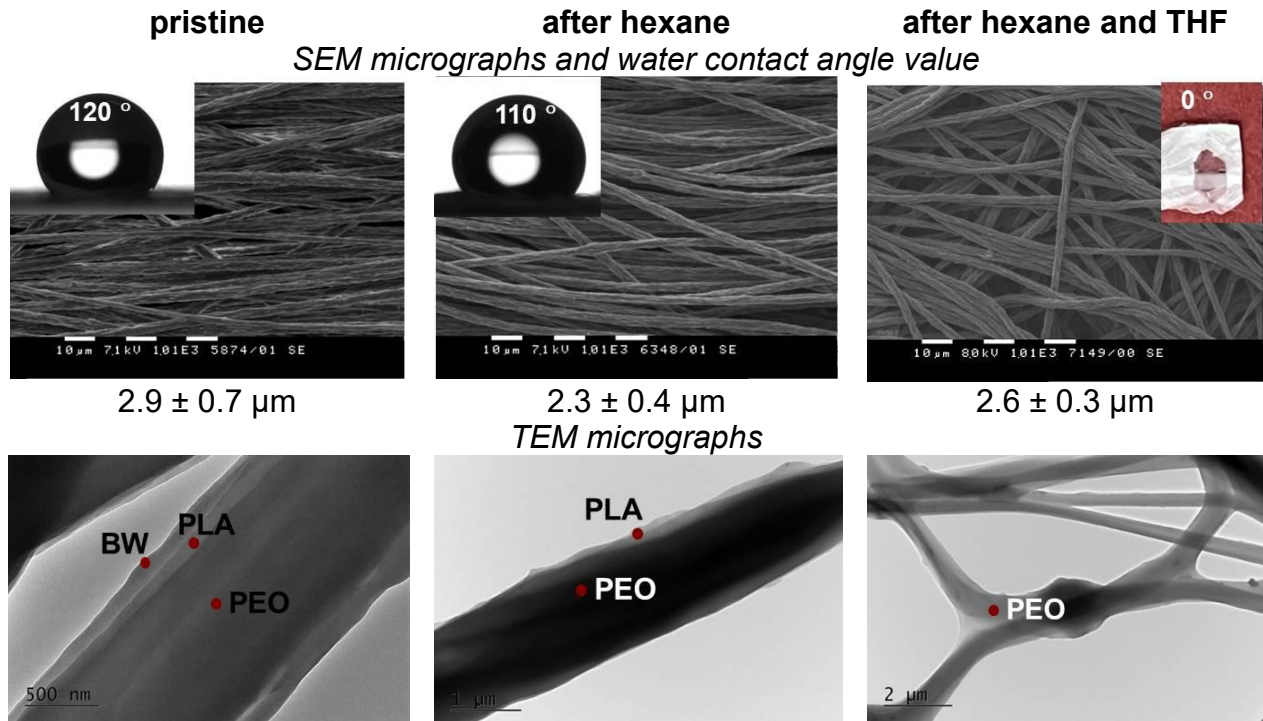


Figure G3-6. SEM and TEM micrographs of a mat and of single fibers from PEO/PLA/BW before and after sequential selective extraction with hexane and THF. The mean fiber diameters determined from the SEM micrographs are indicated. The measured water contact angles before and after sequential selective extraction with hexane and THF are also shown. Magnification of SEM micrographs: $\times 1,000$; magnification of TEM micrographs: $\times 10,000$ (initial and after hexane treatment) or $\times 2,500$ (after sequential treatment with hexane and THF).

TEM analysis confirmed the preservation of the core–sheath structure (**Figure 3-4**), while the FTIR spectra exhibited a characteristic band at 1722 cm^{-1} (stretching vibration of the ester C=O group of PHB) (**Figure 3-5** in the dissertation), confirming the presence of a second sheath of PHB. In contrast, in mats containing polyesters readily soluble in THF, such as PCL, PLAGA, and PLA, the weight loss coincided with the theoretical value, and the fibers became completely hydrophilic, with a recorded water contact angle of 0° (**Figure 3-6**). TEM micrographs revealed only monolithic PEO fibers (**Figure 3-6**), and the FTIR spectra after sequential extraction with hexane and THF

matched those of PEO (**Figure 3-7**). This confirms the removal of the inner sheath. XRD analysis showed an overlap of some of the diffraction peaks of the polyesters with those of PEO and beeswax. Regarding thermogravimetric analysis, no changes were observed in the thermal decomposition of the components (PEO, polyester, and beeswax) of the composite fibrous materials.

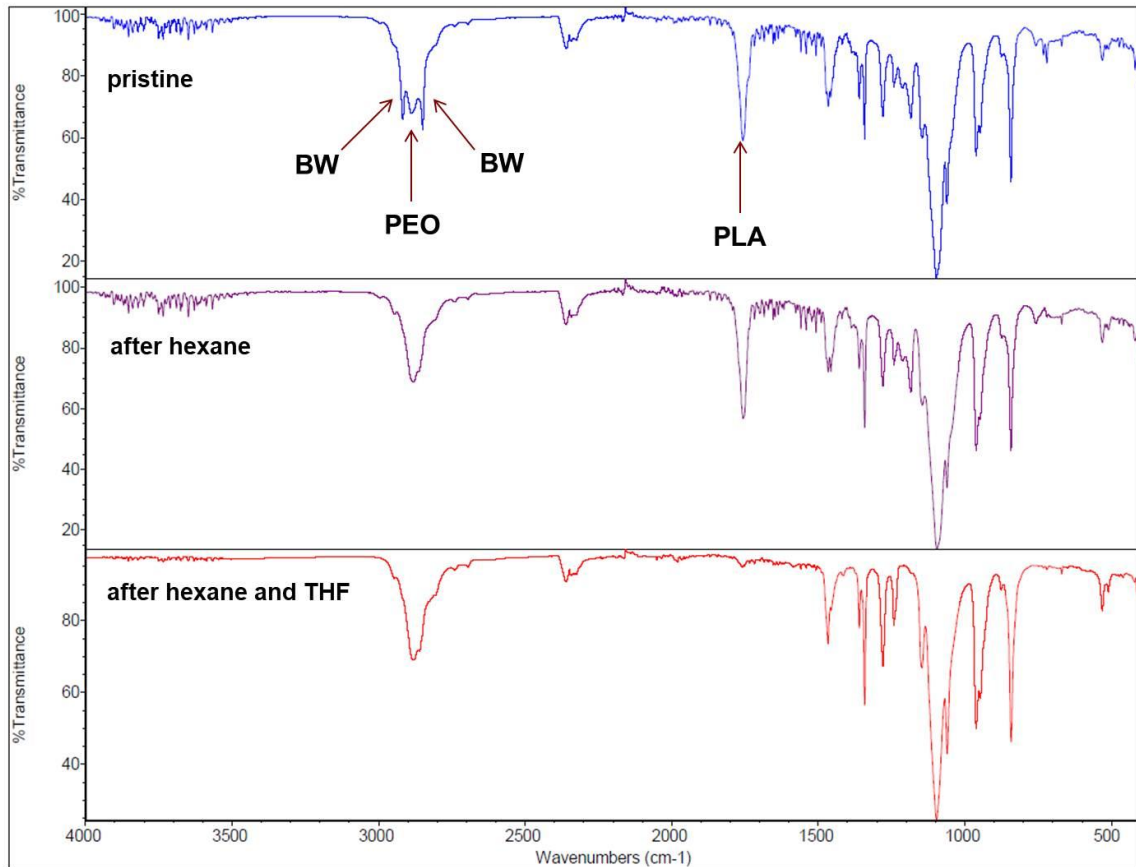


Figure G3-7. Comparison of the FTIR spectra of a fibrous material of PEO600k/PLA/BW before and after extraction with hexane (24 h) or after sequential extraction with hexane and THF (4 h).

The mechanical tests demonstrated that the mechanical properties strongly depended on the type of polyester used (**Figure G3-8** in the dissertation). PEO600k/PLA259k/BW and PEO600k/PCL/BW mat exhibited the highest elasticity (elongation >200%), whereas PEO600k/PHB/BW mat were the most brittle (elongation ~50%). The highest tensile strength and Young's modulus were recorded for PEO600k/PLA259k/BW mat (~5.5 MPa and ~430 MPa).

3.1.2. Core–double sheath fibers obtained using a polyester with a molar mass higher than that of PEO

After the successful preparation of core-double sheath fibers using polyesters with molar mass lower than that of PEO600k, we investigated what occurred when the polyester used has a higher molar mass than PEO. Two types of experiments were performed: 1. Replacement of PEO600k with PEO100k while keeping the polyester as PLA259k; 2. Replacement of PLA259k with PLA911k while keeping PEO600k.

It was found that replacing PEO600k with PEO100k while using PLA259k did not alter the architecture of the PEO/PLA/BW fibers, which remained core-double sheath ones (**Figure G3-9** in the dissertation). The mats were hydrophobic, with a water contact angle of $110 \pm 4.43^\circ$. After hexane extraction, the weight loss was close to the theoretical value, and the FTIR spectrum showed the absence of characteristic BW bands at 2915 and 2848 cm^{-1} , confirming the removal of the outer sheath (**Figure G3-10** in the dissertation). The water contact angle after hexane extraction decreased to $90.0 \pm 4.11^\circ$, suggesting that the inner sheath consisted mainly of PLA with traces of PEO. Subsequent extraction with THF enabled the removal of the hydrophobic fraction of PLA. Evidence for this was the complete hydrophilization of the mats, with a water contact angle of 0° . However, the FTIR spectrum of the PEO100k/PLA259k/BW mat displayed a weak band at 1759 cm^{-1} , characteristic of the carbonyl group of the ester moiety of PLA. This indicates that the fiber core was composed mainly of PEO but contained traces of PLA. The reason lies in the higher mobility of PEO100k, which can migrate into the sheath, and the lower mobility of PLA259k, which remains partly in the core.

A similar mixing of the components was also observed in the second group of experiments, in which PEO600k was retained while PLA259k was replaced with the higher molar mass polylactide PLA911k. As seen in the TEM micrograph in **Figure G3-11**, the core-double sheath architecture was preserved. After hexane extraction, the outer BW sheath was removed, which was confirmed by FTIR analysis by the absence of the characteristic BW bands (**Figure G3-12** in the dissertation). The water contact angle of the mat decreased to 90° , suggesting that the inner sheath contained PLA with incorporated PEO chains. After extraction with THF, monolithic fibers were obtained, but no significant change in the contact angle was detected, remaining at ca. 60° . This

indicates that PLA911k, due to its high molar mass and lower mobility, was unable to fully migrate into the sheath and remained partially in the core.

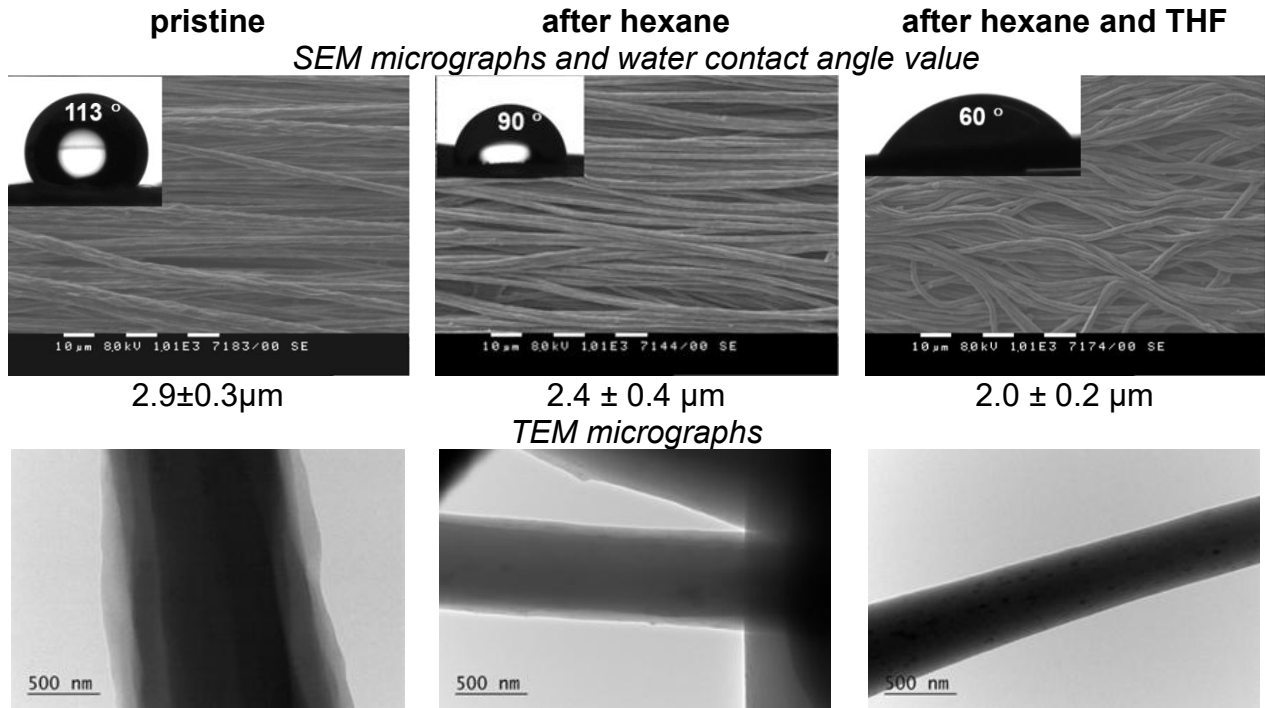


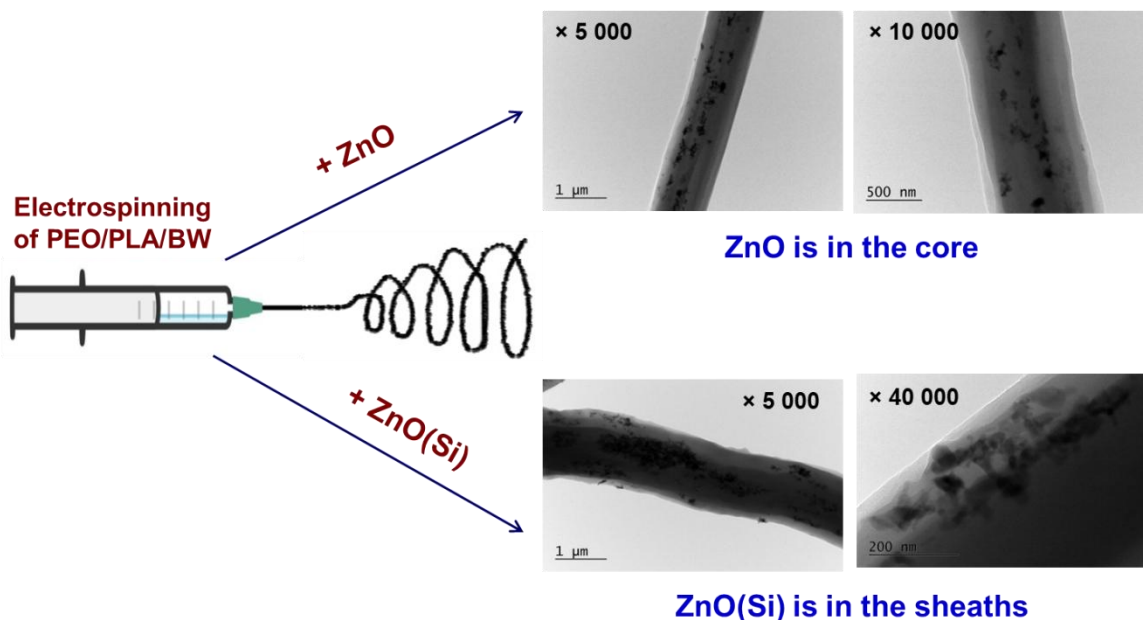
Figure G3-11. SEM and TEM micrographs of a mat and of single fibers from PEO600k/PLA911k/BW before and after sequential selective extraction with hexane and THF. The mean fiber diameters determined from the SEM micrographs are indicated. The measured water contact angles before and after sequential selective extraction with hexane and THF are also shown. Magnification of SEM micrographs: $\times 1,000$; magnification of TEM micrographs: $\times 10,000$.

On the other hand, the lower molar mass of PEO600k, and consequently its higher mobility compared to PLA911k, allowed some of its polymer chains to participate in the formation of the inner sheath of the PEO600k/PLA911k/BW fibers with a core-double sheath architecture.

3.2. Core–double shell fibers of PEO/PLA/BW/ZnO and PEO/PLA/BW/ZnO(Si)

In order to evaluate the possibility of targeted one-step incorporation of a hydrophobic or hydrophilic low-molecular-weight bioactive agent during the electrospinning of homogeneous PEO600k/PLA259k/BW solutions into the hydrophilic core or into the hydrophobic sheaths, respectively, hydrophilic nanosized ZnO with an unmodified surface and hydrophobic nanosized ZnO(Si) with a silanized surface were used as model nanoscale contrast markers with bioactive properties. They were added

to the homogeneous solutions of PEO600k/PLA259k/BW, and the resulting suspensions were subjected to electrospinning. As shown in the TEM micrographs in **Scheme G3-2**, the presence of ZnO and ZnO(Si) did not alter the fiber architecture: the fibers retained their core–double sheath structure.



Scheme G3-2. Schematic representation of the preparation of mats from PEO600k/PLA259k/BW/ZnO or PEO600k/PLA259k/BW/ZnO(Si) suspensions and TEM micrographs showing the localization of hydrophilic ZnO or hydrophobic ZnO(Si) in the fibers from PEO600k/PLA259k/BW/ZnO or PEO600k/PLA259k/BW/ZnO(Si).

The difference lay in the distribution of ZnO and ZnO(Si) within the fiber structure. During electrospinning, hydrophilic ZnO preferentially localized in the hydrophilic PEO core of the fibers, while hydrophobic ZnO(Si) was distributed in the hydrophobic sheaths of the fibers (**Scheme G3-2**). These results demonstrate that the selection of a hydrophilic and a hydrophobic contrast marker was appropriate for visualizing the possibility of targeted one-step location of a hydrophilic or hydrophobic low-molecular-weight additive (including a drug) during the single-nozzle spinneret electrospinning of homogeneous PEO600k/PLA259k/BW solutions into the core or into the sheaths, respectively, of the resulting fibers.

3.3. Composite fibrous materials of PEO/polyester/BW with incorporated NQ or CQ

Fibers of PEO600k/PLA259k/BW/CQ and PEO600k/PCL/BW/NQ were obtained and characterized at a drug content of 10 wt.% and at PEO/polyester/BW = 60/20/20 (w/w). The presence of CQ or NQ led to the formation of fibers with whiskers along the main fibers (**Figure G3-14** in the dissertation). The average diameter of the main fibers was about $1.90 \pm 0.19 \mu\text{m}$, while that of the whiskers was $0.40 \pm 0.07 \mu\text{m}$. TEM micrographs demonstrated that even with the addition of the drug, the fibers retained their core-double sheath architecture.

The release values of NQ (%) were compared for the following mats: PEO600k/BW/NQ (core-sheath fibers), PEO600k/PCL/NQ (core-double sheath fibers), and PEO600k/PLA/NQ (core-double sheath fibers) (**Figure G3-16** in the dissertation). During the initial release stage (5 min), the material composition did not significantly alter the amount of released NQ, which was less than 30%. In the subsequent stage (up to 60 min), however, the material composition affected the release, which decreased in the following order: PEO600k/BW/NQ > PEO600k/PCL/NQ > PEO600k/PLA259k/NQ. This demonstrated that the presence of an inner polyester sheath in the core-double sheath fibrous materials PEO600k/PCL/NQ and PEO600k/PLA259k/NQ slowed down NQ release within this time frame, with a stronger delay observed for PEO600k/PLA/NQ compared to PEO600k/PCL/NQ. NQ was completely released from PEO600k/BW/NQ and PEO600k/PCL/NQ after 90 min, while for PEO600k/PLA/NQ the released amount was ca. 65%. These results indicated that drug release could be modulated by selecting both the fiber architecture and the polyester used to form the inner sheath of the PEO/polyester/BW/NQ core-double sheath fibers.

In Chapter 3, it is demonstrated that the method proposed in Chapter 2 for obtaining fibers with a core-double sheath architecture is also applicable when using other biodegradable aliphatic polyesters. By analogy with the PEO/PLA/BW system, it was shown that fibers from PEO/polyester/BW preserve the same architecture. The sequential removal of the outer and inner sheaths by selective extraction was traced, revealing that the outer layer consisted of BW, while the composition of the inner sheath and the core depended on the molar mass ratio of the polyester and PEO. When the polyester had a lower molar mass than PEO, the inner sheath was composed solely of

the polyester, and the core solely of PEO. When the polyester had a higher molar mass than PEO, the inner sheath was composed mainly of the polyester with traces of PEO, while the core consisted predominantly of PEO with traces of polyester. Appropriate contrast agents: hydrophilic ZnO and hydrophobic ZnO(Si), were found for demonstration the possibility of directed deposition of hydrophilic or hydrophobic bioactive agents into the core or into the sheaths, respectively, of PEO/polyester/BW fibers during the electrospinning process. The studies on NQ release from the fibrous materials revealed that, in the initial stages of release, it depends both on the fiber architecture (core-sheath or core-double sheath) and on the molar mass of the polyester forming the inner sheath of the PEO/polyester/BW/NQ fibers.

Chapter 4. Antibacterial, Antifungal, and Anticancer Activity of the Novel Fibrous Materials Containing NQ or CQ [P1 - P4], [OP1,OP2, OP3], [PP1,PP2]

In order to demonstrate the potential applicability of the novel fibrous materials, composed of fibers with a core-sheath architecture (PEO/BW) or a core-double sheath architecture (PEO/PLA/BW or PEO/PCL/BW), as drug carriers with preserved biological activity, we performed a microbiological screening of the above-mentioned mats containing NQ or CQ. It is well known that NQ derivatives exhibit antibacterial and antifungal activity against a wide range of human pathogenic microorganisms. Therefore, in our study, the antibacterial and antifungal activity of the novel NQ-containing mats was evaluated *in vitro* against the following human pathogens: the bacteria *B. cereus*, *E. coli*, *P. aeruginosa*, and *S. aureus*, as well as the fungus *C. albicans*. NQ is a derivative of 8-hydroxyquinoline, which is also reported to exert anticancer effects. For this reason, we further studied the anticancer activity of PEO/BW/NQ mats against the model cancer cell lines HeLa (cervical adenocarcinoma) and SH-4 (human melanoma). Our knowledge that both NQ and CQ exhibit antibacterial and antifungal activity against phytopathogenic microorganisms inspired the idea that the new fibrous materials incorporating one of these 8-hydroxyquinoline derivatives could find application in agriculture. The following model phytopathogens were used: *P. corrugata*, *F. graminearum*, and *F. avenaceum*. In addition, we examined the behavior of the new fibrous materials containing NQ or CQ in contact with plant-beneficial microorganisms, namely *P. chlororaphis*, *B. amyloliquefaciens*, and *T. asperellum*.

4.1. Investigation of the Interactions of the Novel Composite Fibrous Materials Containing NQ with Human Pathogenic Microorganisms

The antibacterial activity of the mats was evaluated by determining the inhibition zones around fibrous discs against the Gram-positive bacterium *S. aureus* and the Gram-negative bacteria *E. coli*, *P. aeruginosa*, and *B. cereus*, while the antifungal activity was assessed against *C. albicans*. It is well established that NQ exhibits antimicrobial activity against these microorganisms, with minimum inhibitory concentrations ranging from 2.4 mg/L to 64 mg/L. Its mechanism of action is associated with the formation of chelate complexes with divalent cations that are essential for the microbial metabolism.

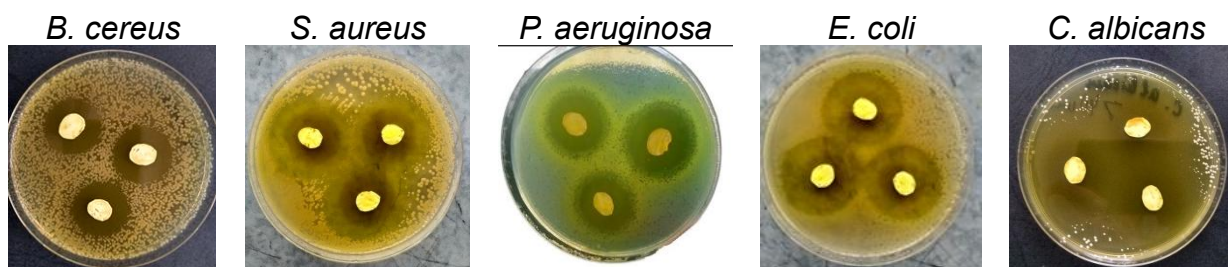


Figure G4-2. Representative digital photographs of the inhibition zones recorded after 24-h exposure of PEO600k/PCL/BW/NQ mats to *B. cereus*, *S. aureus*, *P. aeruginosa*, or *E. coli*, and after 48-h exposure to *C. albicans*.

Upon contact of the control mat PEO(50)/PLA(25)/BW(25) with the microorganisms, no inhibition zones were observed, confirming the lack of activity of PEO, PLA, PCL, and BW (**Figure G4-1** in the dissertation). In contrast, the presence of NQ in the mats of the PEO/BW/NQ, PEO/PLA/BW/NQ, and PEO/PCL/BW/NQ series resulted in clearly distinguishable inhibition zones, as shown in **Figure 4-2**. The inhibition zones determined, for example, for the PEO600k/PCL/BW/NQ mat are presented in **Table G4-1**. As seen, the inhibition zone depends on the type of human pathogenic microorganism used. Similar results were obtained with the other novel fibrous materials. This indicates that NQ, incorporated into fibrous materials with different architectures: core-sheath or core-double sheath, retains its antimicrobial activity. Therefore, the studied novel fibrous materials represent a suitable carrier for this drug and hold potential for medical applications, for example in wound treatment.

Table G4-1. Inhibition zones determined for PEO/PCL/BW/NQ mats after 24-h contact with *B. cereus*, *S. aureus*, *P. aeruginosa*, or *E. coli*, and after 48-h contact with *C. albicans*.

Pathogenic microorganism	Inhibition zone [cm]
<i>Bacillus cereus</i>	2.5
<i>Escherichia coli</i>	3.0
<i>Pseudomonas aeruginosa</i>	2.7
<i>Staphylococcus aureus</i>	3.5
<i>Candida albicans</i>	> 4.0

4.2. Investigation of the Interactions of the Novel Composite Fibrous Materials with the Cancer Cell Lines HeLa and SH-4 and with Normal Human BJ Cells

The anticancer activity of NQ was evaluated against human tumor cell lines (HeLa – cervical adenocarcinoma, SH-4 – melanoma) and the normal human cell line BJ (skin fibroblasts). Literature data indicate strong *in vitro* activity of NQ against several cancer cell lines; however, no information is available regarding its toxicity toward HeLa, SH-4, or BJ cells. Therefore, experiments were conducted with NQ in concentrations ranging from 6.25 to 50.00 $\mu\text{M/L}$, and the IC_{50} values for each line were determined (**Table G4-2** in the dissertation). The lowest IC_{50} values were observed for the tumor cells, while significantly higher values were found for BJ cells, indicating selectivity of NQ toward tumor cells. The calculated selectivity index (SI) confirmed this observation, classifying the action of NQ as selective toward HeLa cells and moderately selective toward SH-4 cells. The PEO/BW/NQ mats demonstrated reduced viability of HeLa and SH-4 cells, but only limited effects on BJ cells. The control mats had no effect on cell viability, confirming the lack of cytotoxicity of PEO and BW. It was further established that the PEO/BW ratio did not significantly affect the activity of NQ, due to the similar release kinetics of the active substance (**Figure G4-3** in the dissertation).

The morphological alterations in control and treated cancer cells HeLa and SH-4 after 24 hours of cultivation in the presence of PEO/BW/NQ mats or an NQ solution were evaluated by fluorescence microscopy (**Figure G4-4**).

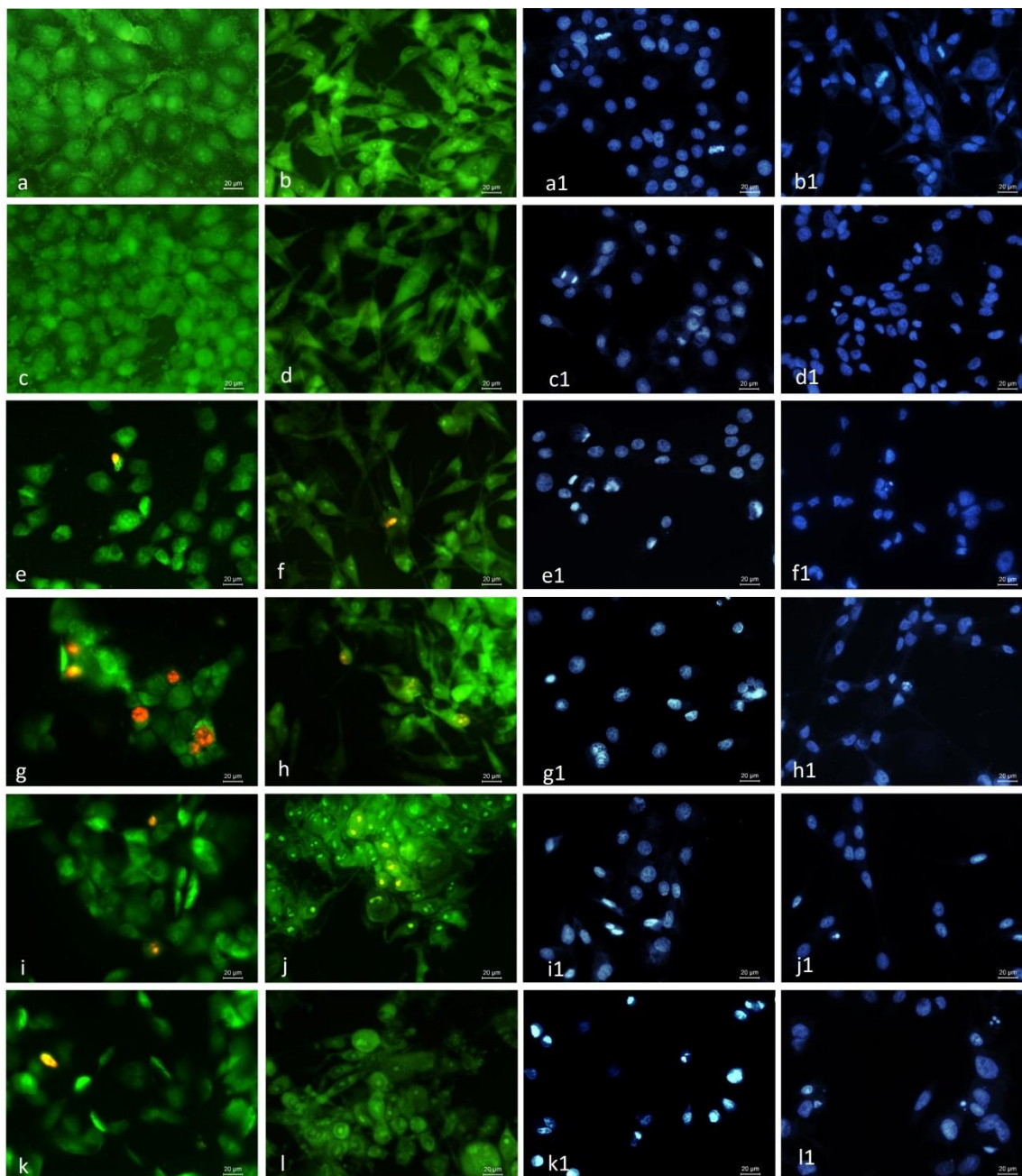


Figure G4-4. Fluorescence micrographs of HeLa (a, c, e, g, i, and k) and SH-4 (b, d, f, h, j, and l) cells stained with AO/EtBr, and HeLa (a1, c1, e1, g1, i1, and k1) and SH-4 (b1, d1, f1, h1, j1, and l1) cells stained with DAPI, incubated in the presence of different fibrous materials or an NQ solution for 24 h. NQ concentration in the fibers or solution = 16 μ M/L. Controls: untreated HeLa (a, a1) and SH-4 (b, b1) cells. Fibrous materials: PEO(70)/BW(30) (c, d, c1, d1), PEO(70)/BW(30)/NQ (e, f, e1, f1), PEO(60)/BW(40)/NQ (g, h, g1, h1), and PEO(80)/BW(20)/NQ (i, j, i1, j1); NQ solution (k, l, k1, l1). Magnification $\times 300$; scale bar = 20 μ m.

It was found that both NQ solutions and PEO/BW/NQ mats induced apoptosis in tumor cells, as evidenced by nuclear fragmentation, membrane blebbing, chromatin condensation and margination, as well as the formation of apoptotic bodies. In contrast, the control samples did not cause such alterations. This demonstrates that NQ retains its antitumor activity after incorporation into the fibers and exerts its effect through the induction of apoptosis, highlighting the potential of these mats as selective anticancer drug delivery systems.

4.3. Evaluation of the Interactions of the Novel Composite Fibrous Materials with Phytopathogenic and Plant-Beneficial Microorganisms

4.3.1. Interactions of the Novel Fibrous Composites with Phytopathogenic Bacteria and Fungi.

The following phytopathogenic microorganisms were used: *Pseudomonas corrugata* (bacterium), *Fusarium graminearum* and *Fusarium avenaceum* (filamentous fungi), which are among the major causes of severe agricultural damage and are capable of producing mycotoxins harmful to humans. Literature data on the activity of NQ and CQ against these microorganisms are scarce, with the exception of *F. graminearum*. Using the disc-diffusion method with filter paper discs impregnated with NQ or CQ solution, it was found that NQ exhibited pronounced antibacterial and antifungal activity, with inhibition zones of ca. 5.90 ± 0.20 , 5.60 ± 0.40 , and 5.20 ± 0.20 cm for the three phytopathogens. CQ showed lower antibacterial activity against *P. corrugata*, with an inhibition zone of 1.90 ± 0.30 cm. This difference is attributed to the lower solubility of CQ compared to NQ in aqueous medium (**Figure G4-5** in the dissertation). In the next stage, mats from the series PEO/BW/NQ and PEO/PLA/BW/NQ, as well as PEO/PCL/BW/NQ and PEO/PLA/BW/CQ, were subjected to microbiological testing against *P. corrugata* and the fungi *F. graminearum* and *F. avenaceum*. As shown in **Figure G4-6**, no inhibition zones were observed for the control mats, indicating that PEO, PCL, PLA, and BW do not possess antibacterial or fungicidal activity. The presence of NQ in the PEO60/PCL20/BW20/NQ mats induced the formation of clearly distinguishable inhibition zones (**Figure G4-6**, bottom row). In contrast, the mats containing CQ exhibited limited activity, with the largest inhibition zone observed against *P. corrugata* (2.7 ± 0.10 cm). This can be attributed to the poor solubility of CQ in aqueous medium, which hinders its diffusion through the agar and,

consequently, its contact with the cells of the pathogenic microorganisms (**Figure G4-7** and **Table G4-3** in the dissertation).

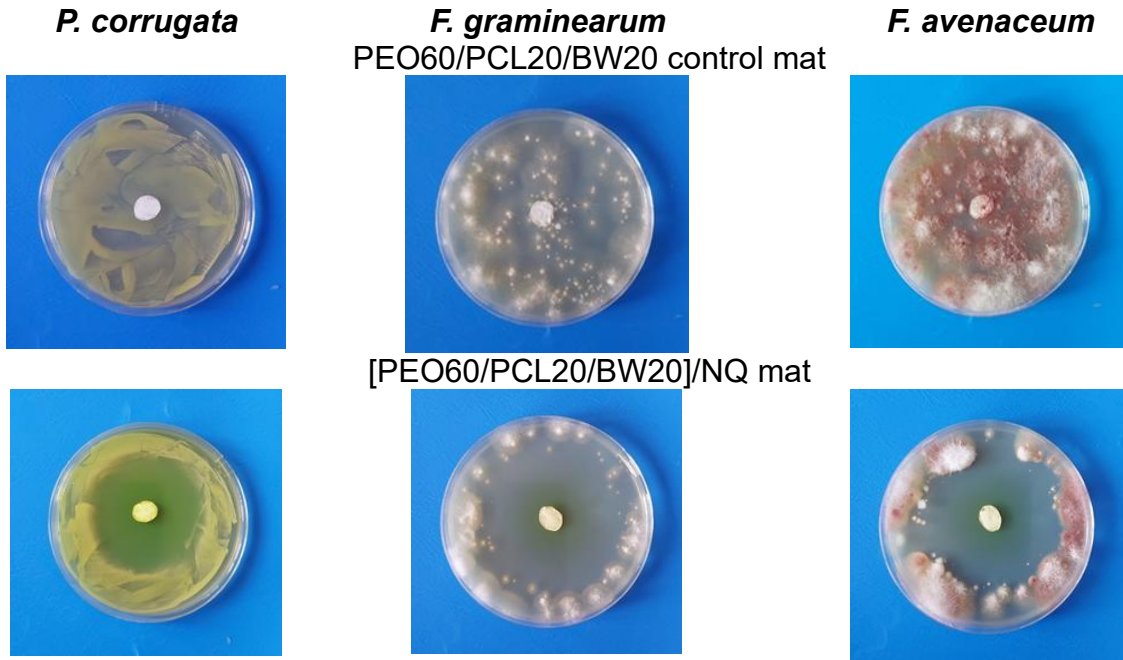


Figure G4-6. Digital photographs of the inhibition zones after contact of fibrous materials PEO(60)/PCL(20)/BW(20)/NQ with phytopathogenic microorganisms (bottom row). For comparison, digital photographs are also shown after contact of the control fibrous materials PEO(60)/PCL(20)/BW(20) with phytopathogenic microorganisms (top row). Left column: *P. corrugata*; middle column: *F. graminearum*; right column: *F. avenaceum*.

4.3.2. Evaluation of the Interactions of the Novel Composite Fibrous Materials with Plant-Beneficial Bacteria and Fungi

The following plant-beneficial microorganisms were used: *Pseudomonas chlororaphis*, *Bacillus amyloliquefaciens*, and *Trichoderma asperellum*, which are among the most widely applied agents in commercial bioproducts for plant protection. Due to the lack of literature data on the effects of NQ and CQ on these beneficial microorganisms, a disc-diffusion assay was performed using filter paper discs impregnated with NQ and CQ solutions. It was found that NQ exhibited antibacterial and antifungal activity against all three microorganisms, with inhibition zones of 4.40 ± 0.10 cm for *P. chlororaphis*, 4.60 ± 0.10 cm for *B. amyloliquefaciens*, and 5.70 ± 0.10 cm for *T. asperellum*. CQ demonstrated limited activity, with smaller inhibition zones - 1.30 ± 0.10 cm and 1.80 ± 0.10 cm against *P. chlororaphis* and *B. amyloliquefaciens*, respectively (**Figure G4-8** in the dissertation).

In the next stage, fibrous materials from the series PEO/BW/NQ, PEO/PLA/BW/NQ, PEO/PCL/BW/NQ, and PEO/PLA/BW/CQ were tested for their interactions with the same microorganisms. The control mats did not inhibit the growth of the beneficial bacteria and fungi. Incorporation of NQ or CQ into the fibrous materials, however, led to the formation of inhibition zones (**Figures G4-9** and **G4-10** in the dissertation). The smallest inhibition zone diameters were recorded for the PEO60/PLA20/BW20/CQ mats (**Table G4-4** in the dissertation). This result is attributed to the poor solubility of CQ in aqueous medium, which slows its diffusion through the agar and hinders its contact with the cells of the beneficial microorganisms.

A preliminary *in vitro* screening was carried out to assess the applicability of the novel fibrous materials, composed of fibers with a core-sheath (PEO/BW) or core-double sheath (PEO/PLA/BW or PEO/PCL/BW) architecture loaded with the bioactive compounds NQ or CQ, in the fields of medicine and agriculture. Regarding medical applications, the results demonstrated that NQ-containing fibrous mats exhibited pronounced antibacterial, antifungal, and selective anticancer activity. This highlights their potential as drug carriers, for instance in wound treatment or in targeted antitumor therapy. Concerning agricultural applications, it was shown for the first time that NQ- and CQ-containing fibrous materials inhibit the growth of both phytopathogens and plant-beneficial microorganisms. These findings emphasize the need to develop new strategies ensuring selective control over harmful microorganisms without compromising the viability of beneficial microbial agents. The acquired knowledge is valuable both for the scientific community and for practices in sustainable agriculture.

IV. CONCLUSIONS

Novel composite fibrous materials with core-sheath or core-double sheath architecture were prepared by electrospinning of homogeneous solutions of PEO/BW and PEO/polyester/BW systems, respectively, without the use of an auxiliary coaxial electrospinning device. The fiber architecture was confirmed through a combination of advanced analytical methods (SEM, TEM, XPS), as well as by developing a systematic approach for the selective extraction of the outer sheath, the inner sheath, and the fiber

core. Furthermore, several potential applications of the new materials were demonstrated, both in medicine and in the field of sustainable “green” agriculture.

1. For the first time, fibers with core–sheath architecture were prepared by electrospinning of homogeneous solutions of PEO and BW. This was achieved by finding of a common solvent (chloroform) of the two partners, enabling the preparation of a homogeneous solution. It was demonstrated that the novel PEO/BW fibrous materials could serve as carriers of bioactive substances, using NQ as a model drug. The release of NQ from the hydrophobic PEO/BW/NQ fibrous materials was studied with the aid of a specially designed cell.

2. For the first time, fibers with core-double sheath architecture were prepared by electrospinning of homogeneous solutions of PEO, PLA, and BW in their common solvent chloroform. This is the first report on the possibility to fabricate core-double sheath fibers from homogeneous solutions without the use of an auxiliary coaxial electrospinning device, as a result of the self-organization of the partners via phase separation. It was further demonstrated that the incorporation of PLA in the fiber structure improved the mechanical properties of the PEO/PLA/BW mats compared to the PEO/BW fibrous materials.

3. Substitution of PLA with other biocompatible and biodegradable aliphatic polyesters (PCL, PLAGA, PBS, or PHB) confirmed the validity of the proposed approach for obtaining core-double sheath fibers from PEO/polyester/BW systems. It was demonstrated that, unlike the composition of the outer sheath (BW), which does not depend on the molar mass ratio of PEO and the polyester, the compositions of the core and the inner sheath are affected by this ratio. When the molar mass of PEO exceeded that of the polyester, the fiber core is composed solely of PEO, while the inner sheath is formed exclusively by the polyester. Conversely, when the molar mass of PEO was lower than that of the polyester, the core is mainly from PEO with traces of the polyester, whereas the inner sheath is predominantly from the polyester with traces of PEO. Using hydrophilic ZnO or hydrophobic ZnO(Si) as contrast agents, the possibility of targeted

deposition of hydrophilic or hydrophobic bioactive compounds during the electrospinning of PEO/polyester/BW systems was demonstrated.

4. The preliminary *in vitro* screening of the applicability of the obtained series of fibrous materials: composed of fibers with core–sheath (PEO/BW) or core-double sheath (PEO/PLA/BW or PEO/PCL/BW) architectures incorporating the drug substances NQ or CQ; showed their potential applications in medicine and in “green” agriculture.

V. CONTRIBUTIONS OF THE DISSERTATION, OUTLINING SOME DIRECTIONS FOR FUTURE RESEARCH

The design of structures with a hydrophilic core and a hydrophobic sheath (polyesters, beeswax) broadens the scope for incorporating bioactive components with hydrophilic or amphiphilic properties into fibers with a core-sheath architecture. Such additives may include natural phenols containing carboxyl and amino groups, as well as active substances derived from various endemic plants or herbs.

The possibility of obtaining fibers with a hydrophilic core and a hydrophobic beeswax outer sheath opens new opportunities for the incorporation of bioactive substances of animal origin. The produced by bees propolis, along with some of its most prominent components, known for their highly attractive biological activity are of particular interest.

A novel approach for design of fibers with core-sheath architecture from homogeneous solutions has been presented. This approach is applicable to a great variety of biodegradable polyesters, with potential for optimizing mechanical, surface, and biological properties. The proposed materials are promising for applications in biomedicine, pharmacy, and tissue engineering. An unresolved issue concerns the use of copolymers, which could allow fine-tuning of hydrolytic or enzymatic degradation rates according to the requirements of medical or agro-pharmaceutical applications.

The feasibility of producing bioactive fibrous dressings with a complex set of desirable properties through single-nozzle spinneret electrospinning reveals attractive prospects for the development of innovative contactless approaches in medicine and therapeutic cosmetics. In perspective, the deposition of therapeutic dressings onto wound surfaces of complex configuration without direct contact between the physician

(or cosmetologist) and the patient becomes readily achievable. This, in turn, could stimulate the development of simple yet effective portable devices for single-nozzle spinneret electrospinning tailored to the needs of traumatology, surgical practice, and therapeutic cosmetics.

VI. LIST OF THE SCIENTIFIC PUBLICATIONS AND SCIENTIFIC COMMUNICATIONS OF THE DOCTORAL STUDENT

The results of the dissertation have been presented in the following publications and scientific communications:

PUBLICATIONS

[P1] Kyuchyuk S., Paneva D., Karashanova D., Markova N., Georgieva A., Toshkova R., Manolova N., Rashkov I. Core-sheath-like poly(ethylene oxide)/beeswax composite fibers prepared by single-spinneret electrospinning. Antibacterial, antifungal and antitumor activities. *Macromolecular Bioscience* 22, 2200015, 1-14, <https://doi.org/10.1002/mabi.202200015>, 2022. **IF 5.859, Q1**

[P2] Kyuchyuk S., Paneva D., Manolova N., Rashkov I., Karashanova D., Markova N., Core/double-sheath composite fibers from poly(ethylene oxide), poly(L-lactide) and beeswax by single-spinneret electrospinning. *Polymers, Special Issue Electrospinning Techniques and Advanced Textile Materials* 14, 5036, 1-20, 2022. <https://doi.org/10.3390/polym14225036>. **IF 4.967, Q1**; open access.

[P3] Kyuchyuk S., Paneva D., Manolova N., Rashkov I., Karashanova D., Markova N. Composite core-double sheath fibers based on some biodegradable polyesters obtained by self-organization during electrospinning. *Journal of Applied Polymer Science* **2024**, 141, e55179. <https://doi.org/10.1002/app.55179>, **IF 2.8, Q2**.

[P4] Kyuchyuk, S.; Paneva, D.; Manolova, N.; Rashkov, I.; Karashanova, D.; Naydenov, M.; Markova, N. Electrospun Fibers of Biocompatible and Biodegradable Polyesters, Poly(Ethylene Oxide) and Beeswax with Anti-Bacterial and Anti-Fungal Activities. *Materials* **2023**, 16, 4882, <https://doi.org/10.3390/ma16134882> **IF 3.748, Q2**, open access.

[P5] Kyuchyuk, S.; Paneva, D.; Manolova, N.; Rashkov, I. Core–Sheath Fibers via Single-Nozzle Spinneret Electrospinning of Emulsions and Homogeneous Blend Solutions. *Materials* **2024**, 17, 5379. <https://doi.org/10.3390/ma17215379>, **IF 3.748, Q2**, open access.

The doctoral student's works have been cited 20 times in the scientific literature (according to Scopus data, as of August 8, 2025).

SCIENTIFIC COMMUNICATIONS

(the name of the presenting author is underlined)

Oral Communications :

[OP1] S. Kyuchyuk, D. Paneva, D. Karashanova, N. Markova, A. Georgieva, R. Toshkova, N. Manolova, I. Rashkov. Preparation of novel core–sheath composite fibers from polyethylene oxide and beeswax by electrospinning. Thirteenth Scientific Session “Young Scientists in the World of Polymers,” Institute of Polymers, Bulgarian Academy of Sciences, Bulgaria, June 2, 2022.

[OP2] S. Kyuchyuk, D. Paneva, N. Manolova, I. Rashkov, D. Karashanova, M. Naydenov, N. Markova. *Core–sheath and core–double sheath composite fibers prepared by single-spinneret electrospinning*. Scientific Conference “Clean Nature for Health,” September 12, 2023.

[OP3] S. Kyuchyuk, D. Paneva, N. Manolova, I. Rashkov. *One-step preparation of core–sheath microfibers through self-organization during the electrospinning process*. Eighteenth Spring Seminar “Interdisciplinary Chemistry,” April 28–30, 2025.

Poster Communications:

[PP1] S. Kyuchyuk, D. Paneva, D. Karashanova, N. Markova, A. Georgieva, R. Toshkova, N. Manolova, I. Rashkov. *Preparation of novel core–sheath composite fibers from polyethylene oxide and beeswax by electrospinning*. IX ePoster Scientific Session for Students, Doctoral Students, and Young Scientists, University of Chemical Technology and Metallurgy, Bulgaria, November 11, 2022.

[PP2] S. Kyuchyuk, D. Paneva, N. Manolova, I. Rashkov, D. Karashanova, N. Markova. *Core–double sheath fibers from polyethylene oxide, poly(L-lactide), and beeswax obtained through self-organization during solution electrospinning*. Fourteenth Scientific Session “Young Scientists in the World of Polymers,” Institute of Polymers, Bulgarian Academy of Sciences, Bulgaria, June 1, 2023.

AWARDS

Best Presentation Award, Thirteenth Scientific Session “Young Scientists in the World of Polymers,” Institute of Polymers, Bulgarian Academy of Sciences, Bulgaria, 2022.

Award in the competition for young scientists “Academician Ivan Evstratiev Geshov” in the field of Nanosciences, New Materials and Technologies, Bulgarian Academy of Sciences, 2023.

SCIENTIFIC ACTIVITY BEYOND THE DISSERTATION TOPIC:

PATENTS AND UTILITY MODELS

1. I. Rashkov, M. Ignatova, N. Manolova, **S. Kyuchyuk**, Ya. Feodorova, T. Tomova, I. Slavova, M. Argirova. *Compositions of forms for topical application on the skin containing Ginkgo biloba seed extract or a mixture of Ginkgo biloba seed extract and an individual biologically active polyphenolic compound*. Applicants: Institute of Polymers – BAS (50%) and Medical University – Plovdiv (50%), project D01-323/18.12.2019 NNP BioActiveMed. **Granted patent No. 67586** of November 6, **2023**.
2. I. Rashkov, M. Ignatova, N. Manolova, **S. Kyuchyuk**, Ya. Feodorova, T. Tomova, I. Slavova, M. Argirova. *Compositions of forms for topical application on the skin containing Ginkgo biloba seed extract or a mixture of Ginkgo biloba seed extract and an individual biologically active polyphenolic compound*. Applicants: Institute of Polymers – BAS and Medical University – Plovdiv. **Registered utility model No. 4109** of June 11, **2021**.

POSTERS

1. V. Kazanlaklieva, S. Kyuchyuk, D. Paneva, M. Ignatova, N. Manolova, I. Rashkov. *Novel electrospun materials from chitosan and rosmarinic acid: preparation, characterization, and antioxidant activity*. Sixteenth Scientific Session “Young Scientists in the World of Polymers,” March 4, 2025.
2. S. Kyuchyuk, N. Stoyanova, M. Ignatova, N. Manolova, I. Rashkov. *Novel polymeric nanosized systems containing biologically active compounds: preparation and antioxidant activity*. XI Scientific Session “Young Scientists in the World of Polymers,” organized by the Institute of Polymers – BAS, Bulgaria, September 10, 2020.
3. M. Ignatova, I. Rashkov, N. Manolova, S. Kyuchyuk, M. Argirova, A. Georgieva, R. Toshkova. *Innovative electrospun materials containing Ginkgo biloba seed extract with antioxidant and antitumor activity*. Fourth Scientific Conference “Innovative Low-Toxic Biologically Active Agents for Precision Medicine (BioActiveMed),” Banya, Razlog, June 12–16, 2023.

PARTICIPATION IN RESEARCH CONTRACTS:

1. D01-217/30.11.2018 – National Research Program “Innovative Low-Toxic Biologically Active Agents for Precision Medicine (BioActiveMed).”
2. Contract No. КП-06-H89/9 of December 11, 2024, entitled “*Novel electrospun materials with targeted composition and design containing chitosan and bioactive natural acids: preparation, characterization, and biological activity*,” funded by the Bulgarian Science Fund.